Other reference :
ESTEC/Contract N° 4000102571/10/NL/AF
Type :
Description :
Radiation Characterization of LAPLACE/TANDEM RH Optocouplers, Sensors and Detectors
Title of document :
HAS2 NEUTRON DDD Report

	Names	Dates
Prepared by	VAN AKEN Dirk (ON Semiconductor) BEAUMEL Matthieu (SODERN) HERVE Dominique (SODERN)	23/11/2012
Checked by	-	--
Approved by	-	--
Customer approval	-	-

CHANGE RECORD	
Revision	Description of change
A	First issue
B	Added witness part data

TABLE OF CONTENTS

1.SCOPE AND APPLICABILITY

1.1.Scope

This test report presents the result of the neutron irradiation tests of the HAS2 CMOS image sensor performed in the frame of ESTEC contract N°4000102 571/10/NL/AF “Radiation Characterization of Laplace/Tandem RH optocouplers, sensors and detectors”.

The neutron irradiations were performed at the SCK-SCEN of Belgium with the neutron reactor BR1. Radiations were performed the first week of December 2011. The annealing steps at room temperature and elevated temperatures were performed at ON Semiconductor.

1.2.Purpose

The effect of neutron irradiation and the annealing thereof is studied on the HAS2 in the ON and OFF state.

2.REFERENCES

2.1.Applicable documents

[AD 1] ITT 6429 HAS Irradiation Test Plan, PR__00004584, D

2.2.Reference documents

3.ABBREVIATIONS

AD	Applicable Document
APS	Active Pixel Sensor
CDS	Correlated Double Sampling
CMOS	Complementary Metal-Oxide Semiconductor
DC	DateCode
DDD	Displacement Damage Dose
DR	Destructive Readout
DS	Double Sampling
DSNU	Dark Signal Non Uniformity
ECSS	European Cooperation for Space Standardization
EOL	End Of Life
ESA	European Space Agency
FPN	Fixed Pattern Noise
HAS2	High Accuracy STR 2
LET	Linear Energy Transfer
LSB	Least Significant Bit
N/A	Not Applicable
NDR	Non-Destructive Readout
PCB	Printed Circuit Board
RD	Reference Document
SEE	Single Event Effect
SET	Single Event Transient
SEU	Single Event Upset
SEFI	Single Event Failure interrupt
TID	Total Ionizing Dose

4.DEVICE INFORMATION

4.1.HAS2 presentation

The Accuracy STR 2 sensor (HAS2) is a 1024 x 1024 pixel rolling shutter Active Pixel Sensor (APS), featuring a programmable (gain and offset) output amplifier (PGA) and an internal 12 bits ADC.

The CMOS image was sensor designed and manufactured by ON Semiconductor[1] under ESA contract 17235/03/NL/FM for star tracker applications.

The block diagram of HAS2 is presented in Figure 4-1.

Pixel design is based on a photodiode coupled with a three transistor readout circuit. The HAS2 is the descendant from a lineage radiation-hardened by design sensors from ON Semiconductor: the photodiodes includes a doped surface protection layer to prevent the depleted area from reaching the field oxide interface, while the CMOS readout circuitry is designed using enclosed geometry transistor layouts.

The wafers are produced by Plessey Semiconductors[2] on the standard XC035P311 CMOS process (0.35 µm).

In order to reduce the variation in signal offset from pixel to pixel (known as Fixed Pattern Noise, or FPN) typically seen on APS, the HAS2 implements two different noise reduction techniques: Double Sampling (DS) also called Destructive Readout (DR) and Correlated Double Sampling (CDS) also called Non Destructive Readout (NDR). In DR mode, the pixel is reset at the end of the signal integration time in order to sample the pixel reference level. The reference level is subtracted from the signal level in order to cancel the pixel offset. This internal analog operation is performed before digitization. In NDR mode, two images are sampled and digitized: a reference image at the beginning of the integration time, and a signal image at its end. Offset correction must be performed off-chip by subtracting these two images.

A temperature sensor is also integrated on chip, which can be addressed through an internal multiplexer. This MUX can also address analogue inputs to be digitized by the internal ADC.

[1] Formerly Cypress BVBA and Fillfactory.
[2] Formerly X-FAB.

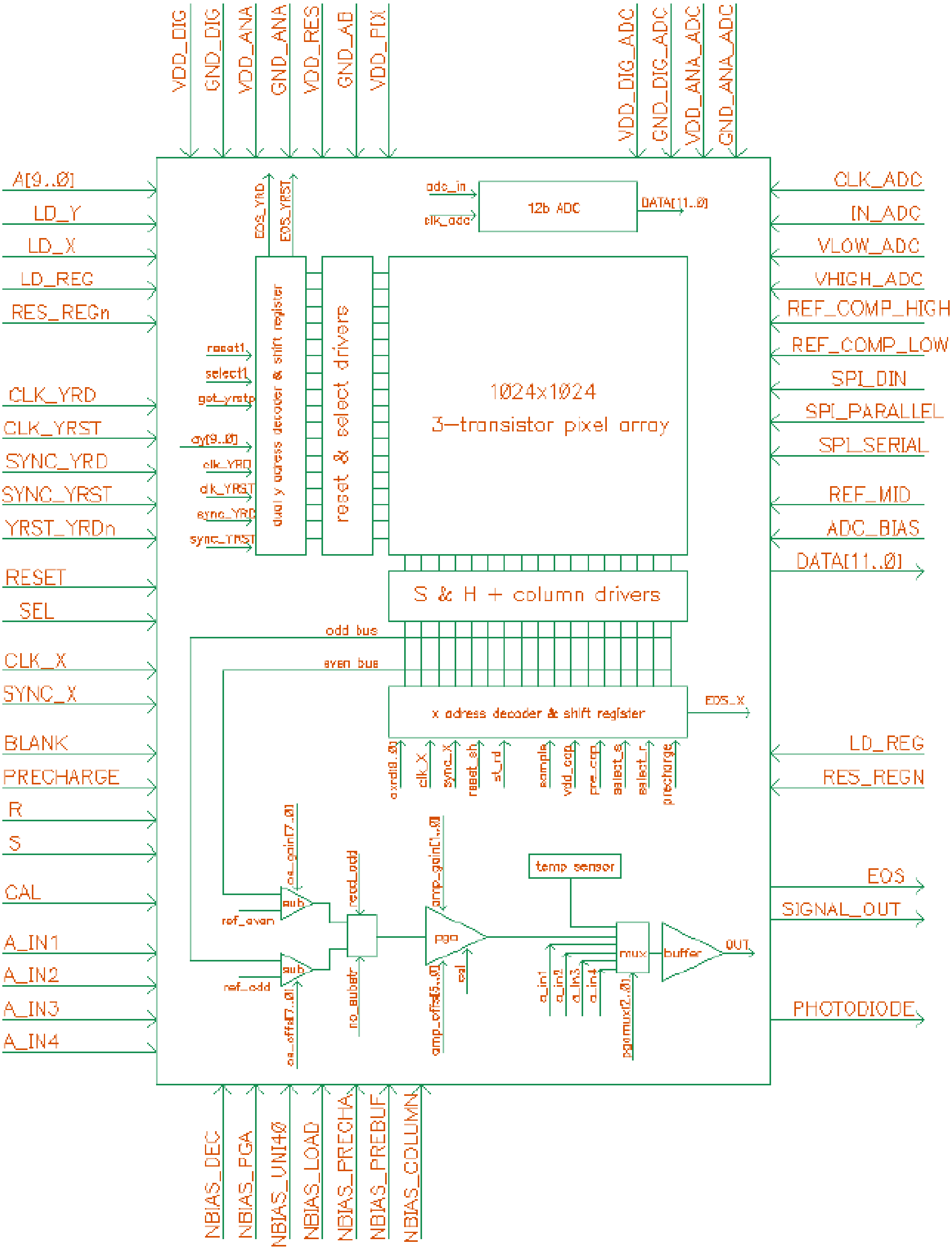

Figure 4-1 : HAS2 block diagram

4.2. Samples identification

Part type: HAS2
Manufacturer: ON Semiconductor
Package: JLCC84
Tested Samples:

164 Reference sample used during HAS ESCC evaluation campaign

722 Sample from wafer lot P29506.1
690 Sample from wafer lot P29506.1
736 Sample from wafer lot P29506.1
703 Sample from wafer lot P29506.1
721 Sample from wafer lot P29506.1
700 Sample from wafer lot P29506.1

712 Sample from wafer lot P29506.1
686 Sample from wafer lot P29506.1
673 Sample from wafer lot P29506.1
707 Sample from wafer lot P29506.1
729 Sample from wafer lot P29506.1
740 Sample from wafer lot P29506.1

Samples from wafer lot P29506.1:
Backside marking: NOIH2SM1000A HHC (Engineering Models)
Date code: 110414 (April 14, 2011)

Samples 700, 729 and 686 were only irradiated till 1.17E+12 neutrons for the purpose of later use during SEE and proton testing.

All samples have been subjected to an operational burn in step at +125 degC during 168h.

5.IRRADIATION FACILITY

Radiations were perfomed at SCK-SCEN in Belgium with the neutron reactor BR1.

Figure 5-1: SCK-SCEN BR1 reactor

More information on the reactor can be found on following website: http://www.sckcen.be/en/Our-Research/Research-facilities/BR1-Belgian-Reactor-1

6. TEST SETUP

The sensors were irradiated in small plastic containers that could hold 6 sensors at a time. The sensors were stacked in the container with conductive foam in between.

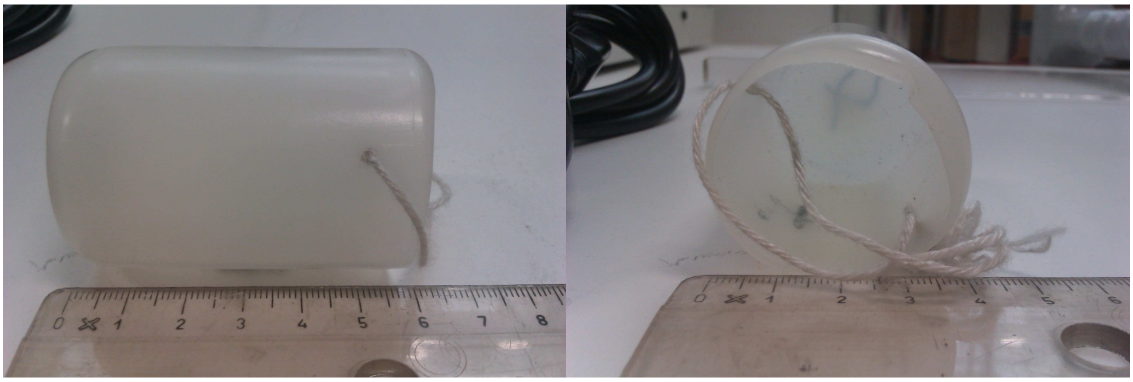

Figure 6-1: plastic bucket used for irradiations

In between the irradiations the sensors were electrically tested using the dedicated HAS2 tester.

7.Test Plan

Electrical measurements are performed at the following steps:

- Initial characterization
- Radiation steps:

Irradiation Time	2’17”	4’33”	15’55”	45’28”	2h39’6”
Fluence	3.9E+10	1.17E+11	3.9E+11	1.17E+12	3.9E+12

⇨ Neutron fluences (1MeV equivalent)/cm^2.

- 3 months room temperature annealing (measurements on a weekly basis)
- 1 month 50 degC annealing (measurements twice a week)
- 168 hours 125 degC annealing (measurements every 24h)

Next to the electrical testing, electro optical testing is performed before the radiation and after $3.9{+}10^{12}$ Neutrons/cm^2.

Devices have been annealed using the following bias conditions:

Condition Item	Bias State during Irradiation test campaign	Bias state during Post irradiation annealing	Serial Numbers
A	OFF	ON	690, 703, 736, 740
B	OFF	OFF	673, 707, 721

Please note that 5 out of the 12 irradiated samples were not subjected to the annealing phase.

Sensors 700, 729 and 686 were used during the proton campaign at PSI. Sensors 712 and 722 were used during the SEE campaign.

8. EXPERIMENTAL RESULTS

8.1. Reported parameters

The following electrical test parameters are reported in the next paragraphs:

- Temporal noise in DR mode (hard reset, hard to soft reset)
- Temporal noise in NDR mode (hard reset, hard to soft reset)
- Offsets (in particular DR mode odd/even offset difference and NDR mode offset dispersion – mean, standard deviation, register value)
- Fixed pattern noise (FPN) local and global (hard reset, hard to soft reset)
- Dark current
- Dark current non uniformity local and global
- Photo response non uniformity local and global
- Temperature sensor output
- Supply currents
- ADC Performances (INL, DNL)

The following electro-optical parameters are measured:

- Spectral Response
- FTM
- Linearity and full well capacity
- Conversion factor
- Dark signal temperature dependency
- Lag performance

8.2.Observations

Reported issues:

1. During room temperature annealing there was some mix-up of the integration time settings between the different running programs. This caused a corruption of the DC data for 5 consecutive weeks at room temperature annealing. This data is removed from the graphs which are shown in the next paragraphs.

2. During 125C annealing the tester was showing some instability. This resulted in some defective columns which were not light responsive anymore. The first thought was that it had to do with the fact that the parts were radiated. However, other un-radiated parts were showing the same issue. Also a replacement of the tester socket and a complete check-up of the system didn't solve the problem. Today, at the moment of writing this report, the issue is still present.

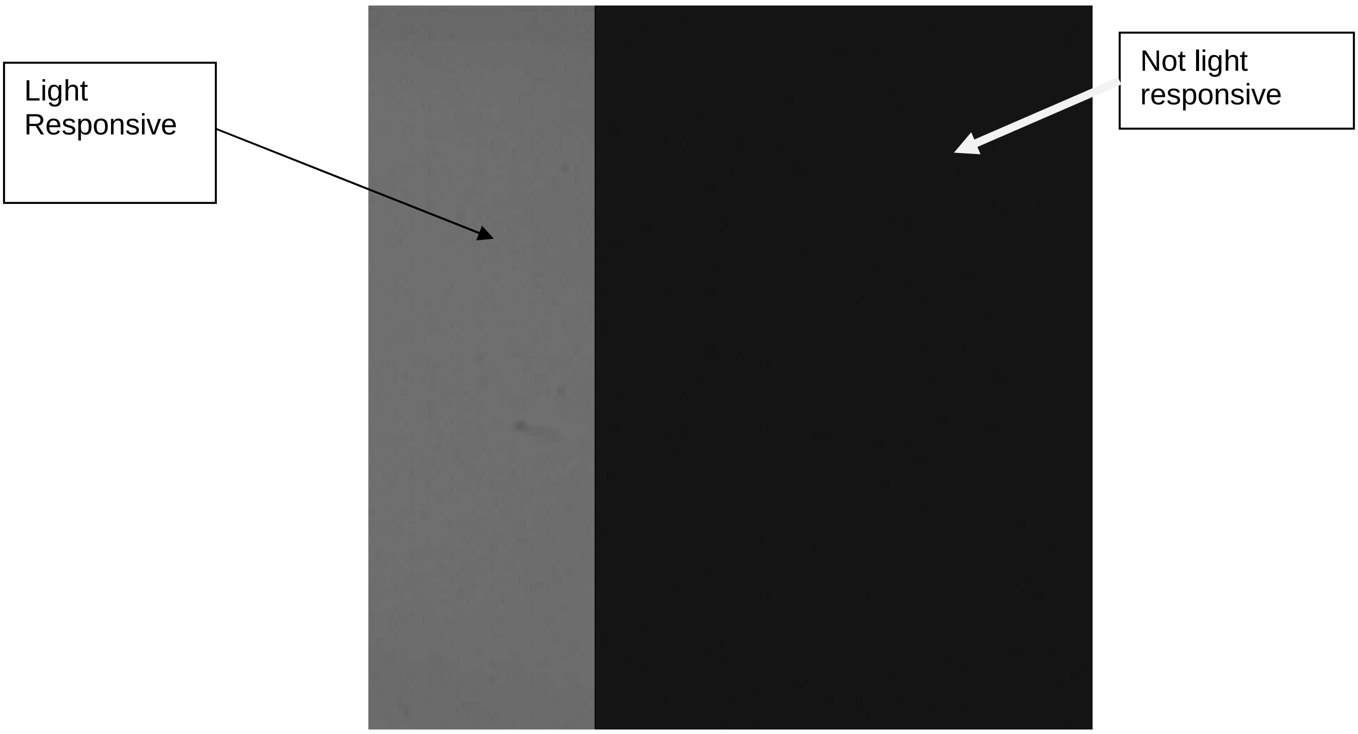

3. In order to have some data available after 125C annealing, the parts were measured on the new HAS2 production tester. Unfortunately most of the test values are not comparable with the ones from the previous tester as in many cases the test method is different. For the most critical parameters like dark current and DSNU we do have these results available.

8.2.1.Dark Current

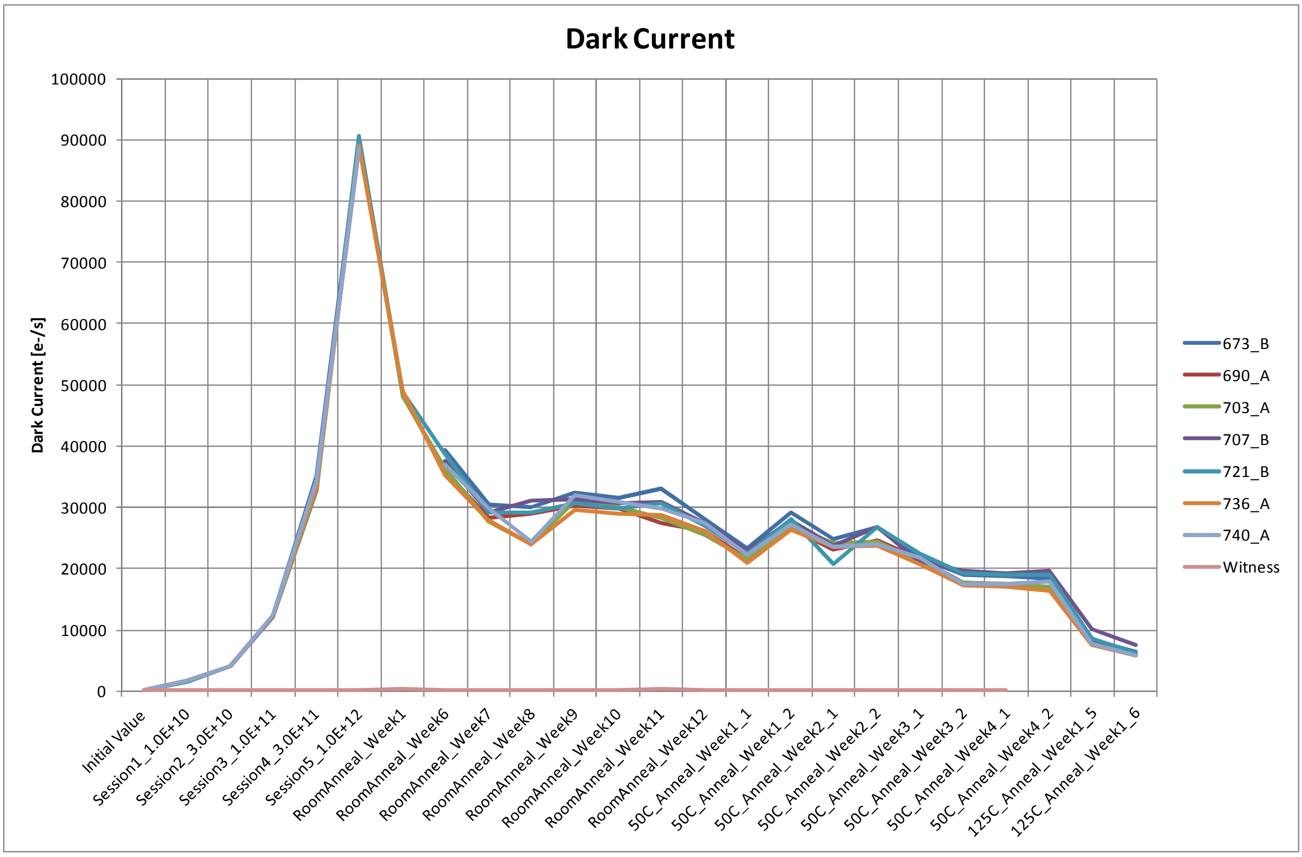

Figure 8-1: Dark Current vs radiation and annealing for different bias conditions

The following observations are made:

- There is almost no spread between the devices during the different irradiation and annealing steps.
- Dark current is saturated after session 5 irradiation.
- Dark current is decreasing rapidly in the first weeks during room temperature annealing.
- Dark current is going down slowly during 50 degrees annealing.
- Dark current is further going down during 125 degrees annealing.
- The type of bias has no influence on dark current behavior during annealing.

8.2.1.1. Dark Current Distributions

The following graphs are showing the distributions for device 740 during the several irradiation steps and annealing steps. Distributions are given for the dark long image and the dark short NDR image. For the dark short NDR image, the raw NDR sample image is given for the first 3 radiation sessions. For all the next sessions and annealing sessions the NDR sample minus reset image is reported.

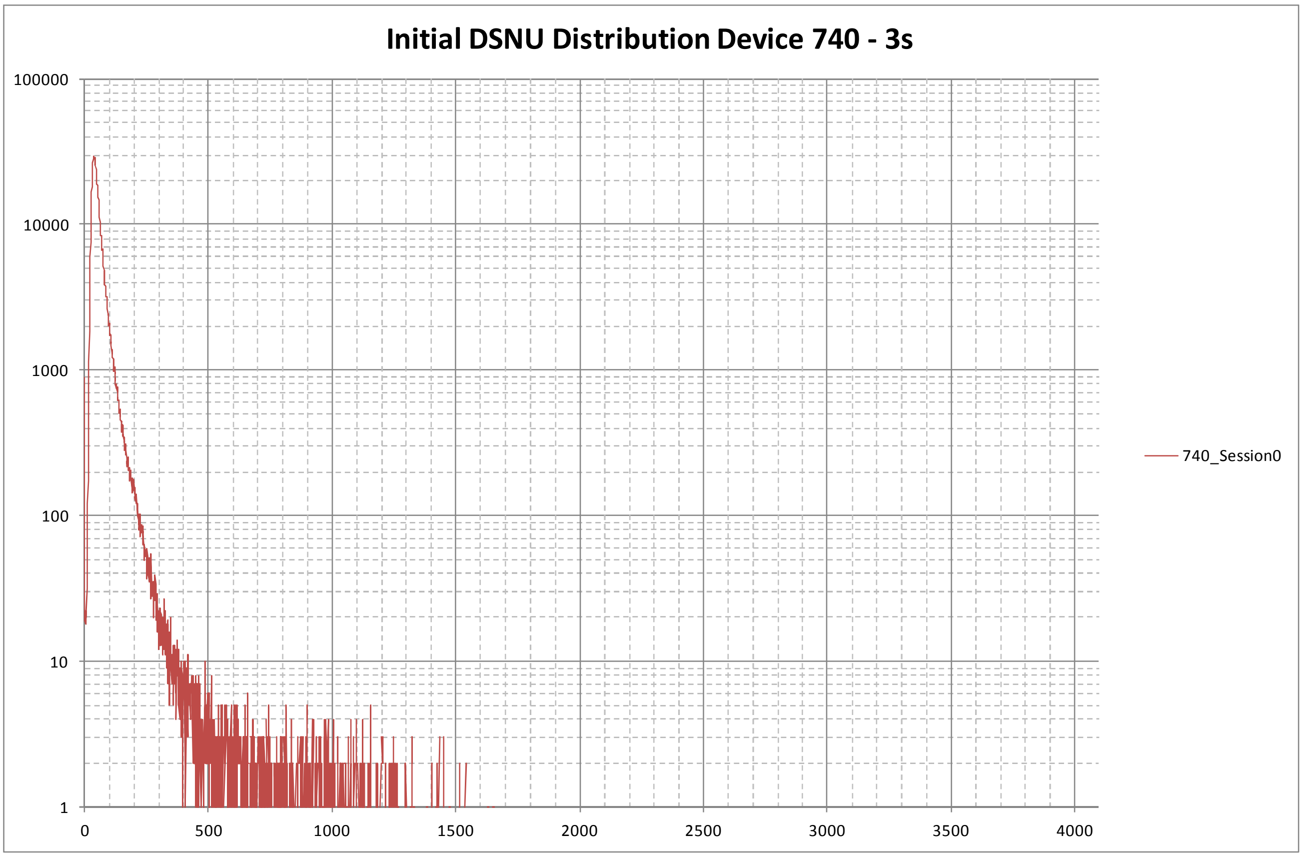

Figure 8-2: Initial DSNU Distribution – Device 740 – 3s

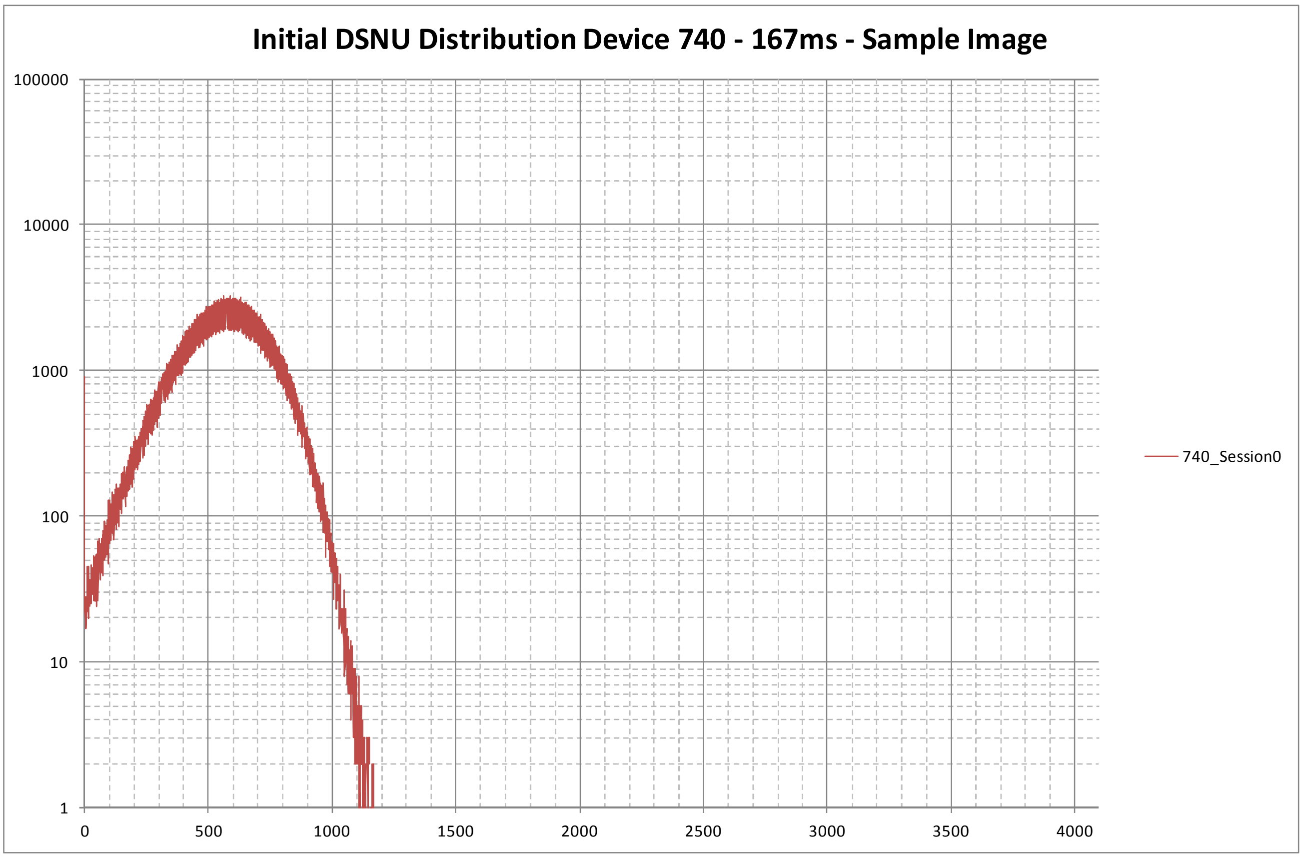

Figure 8-3: Initial DSNU Distribution Device 740 – 167ms – Sample Image

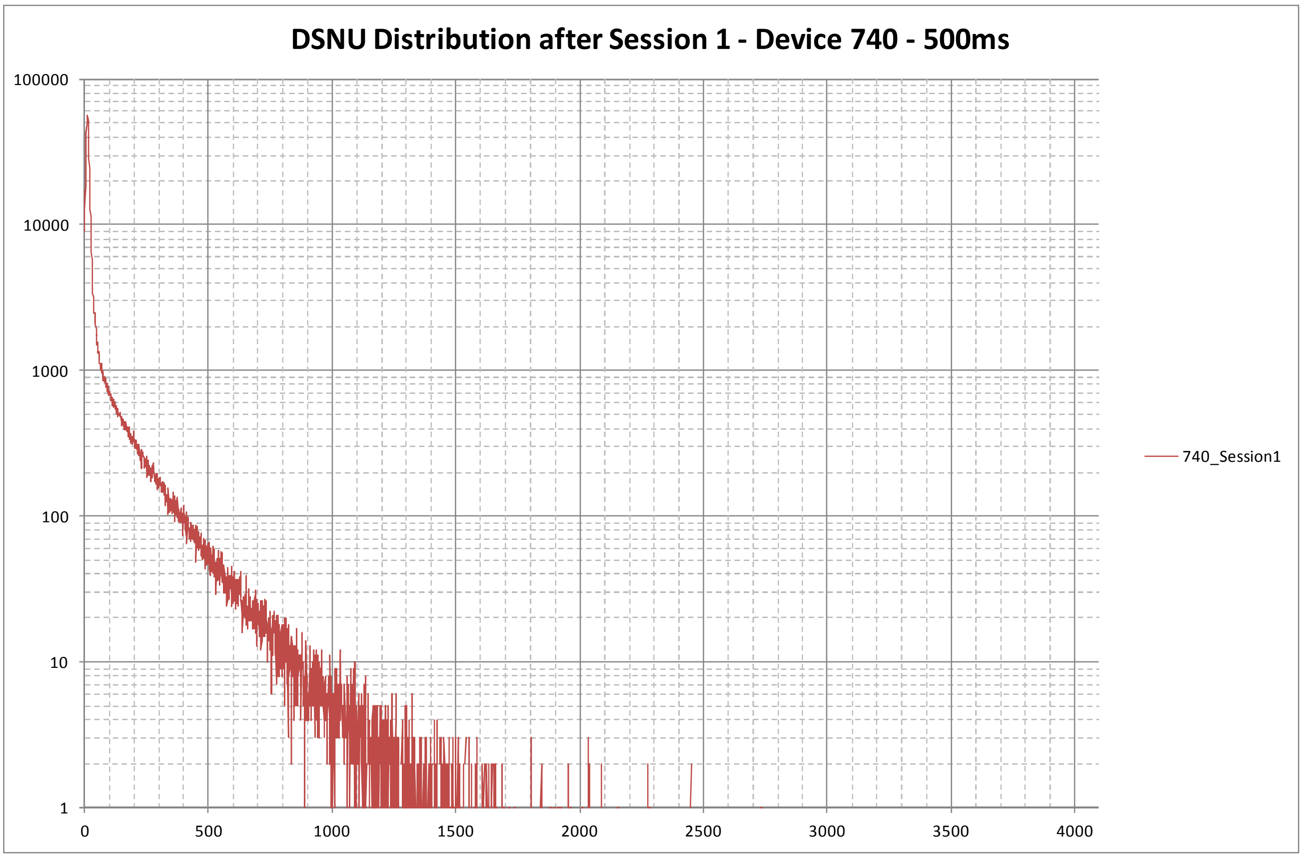

Figure 8-4: DSNU Distribution after Session 1- Device 740 – 500ms

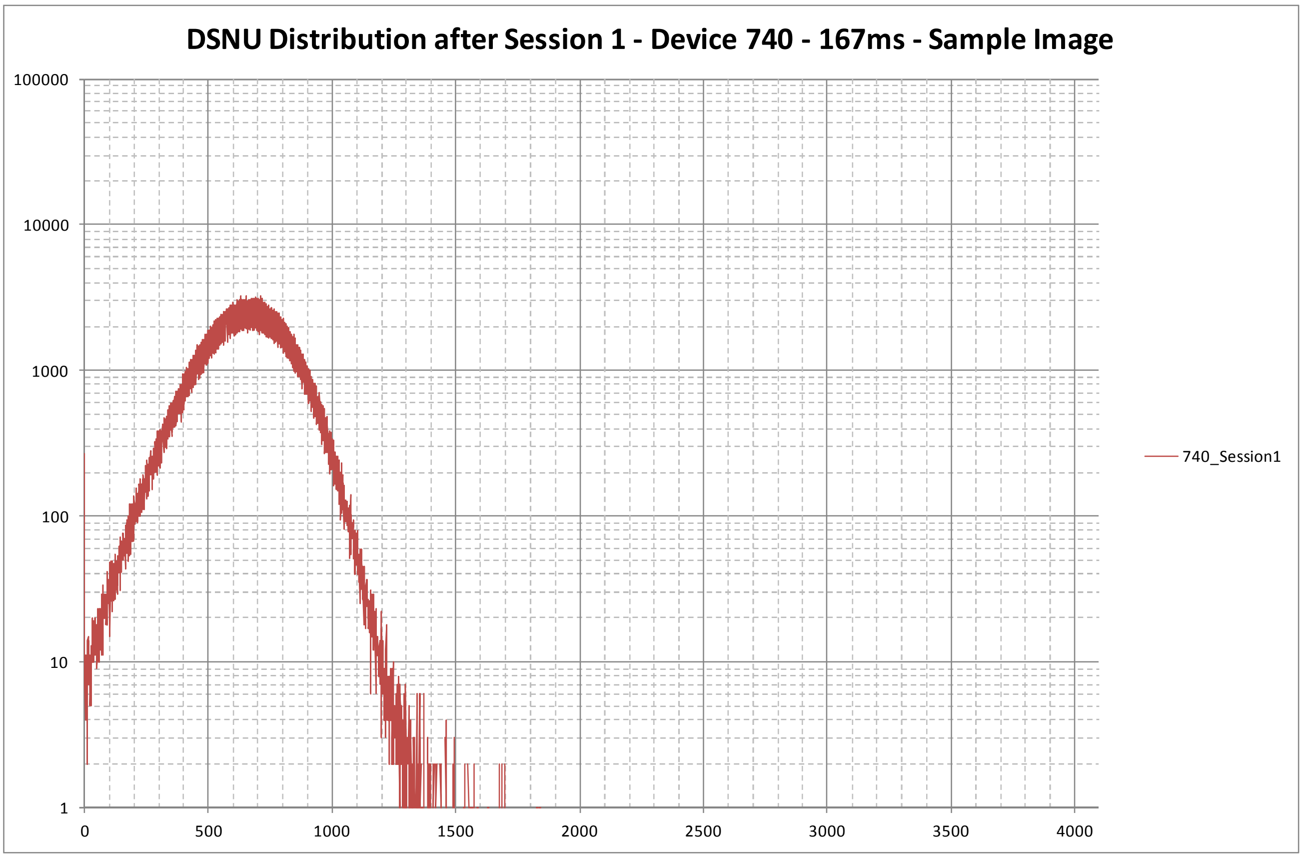

Figure 8-5: DSNU Distribution after Session 1 – Device 740 – 167ms Sample Image

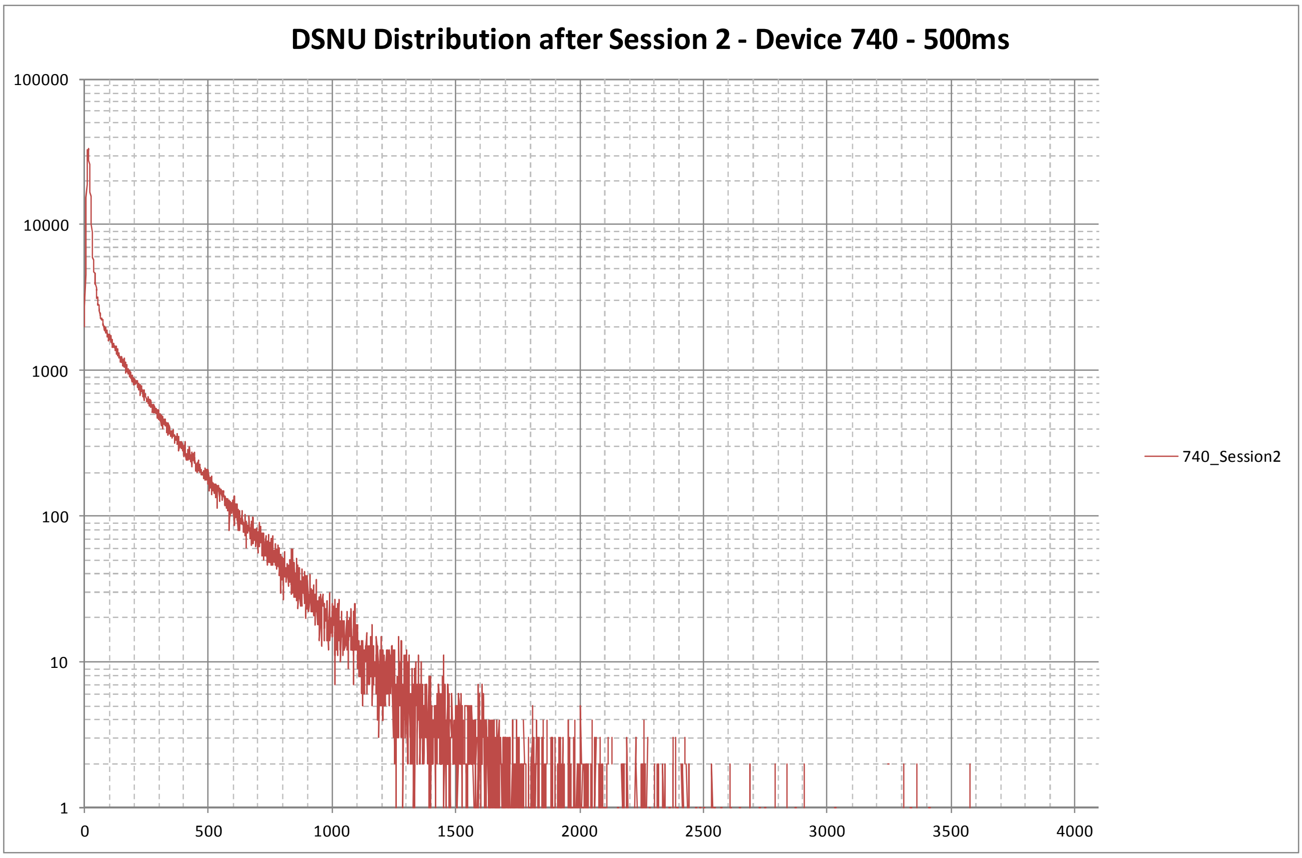

Figure 8-6: DSNU Distribution after Session 2 – Device 740 – 500ms

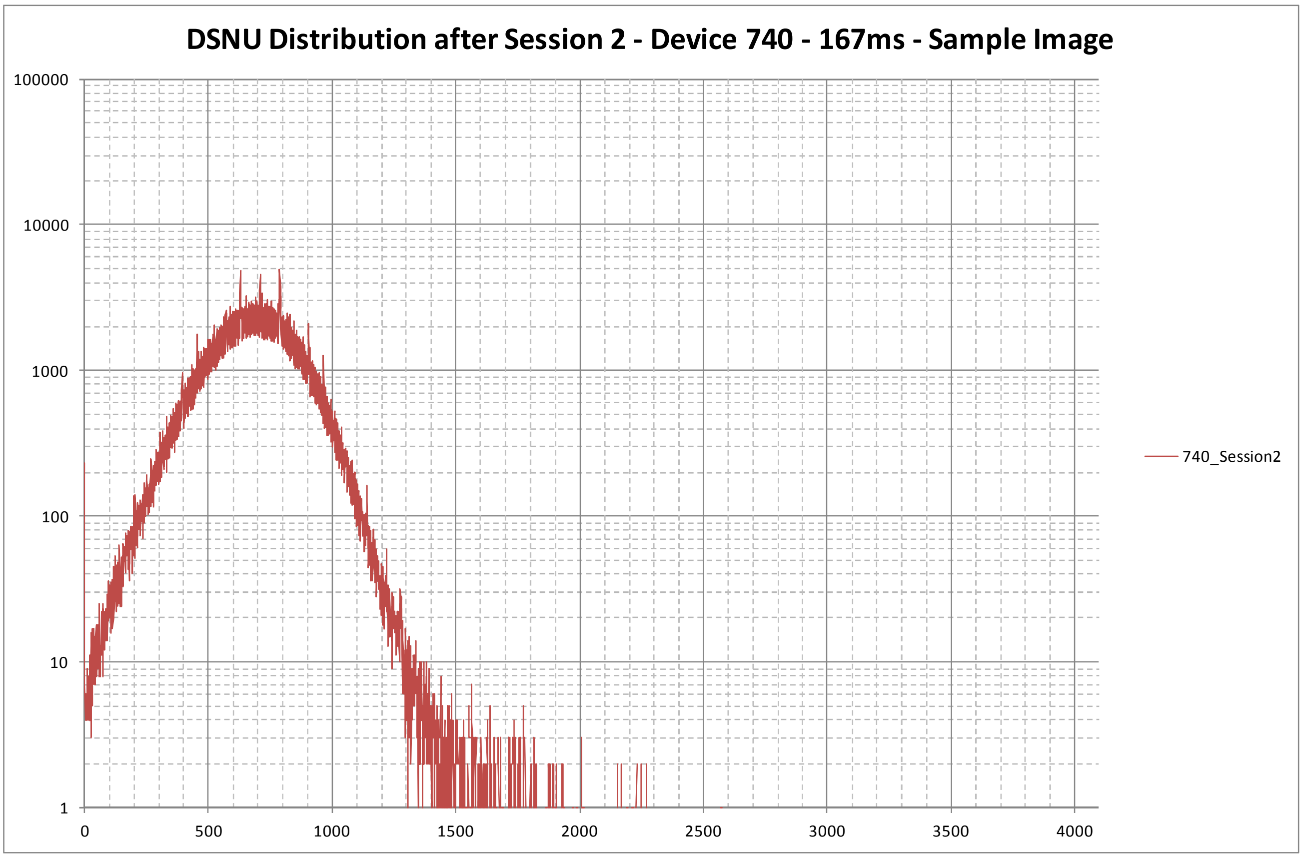

Figure 8-7: DSNU Distribution after Session 2 – Device 740 – 167ms – Sample Image

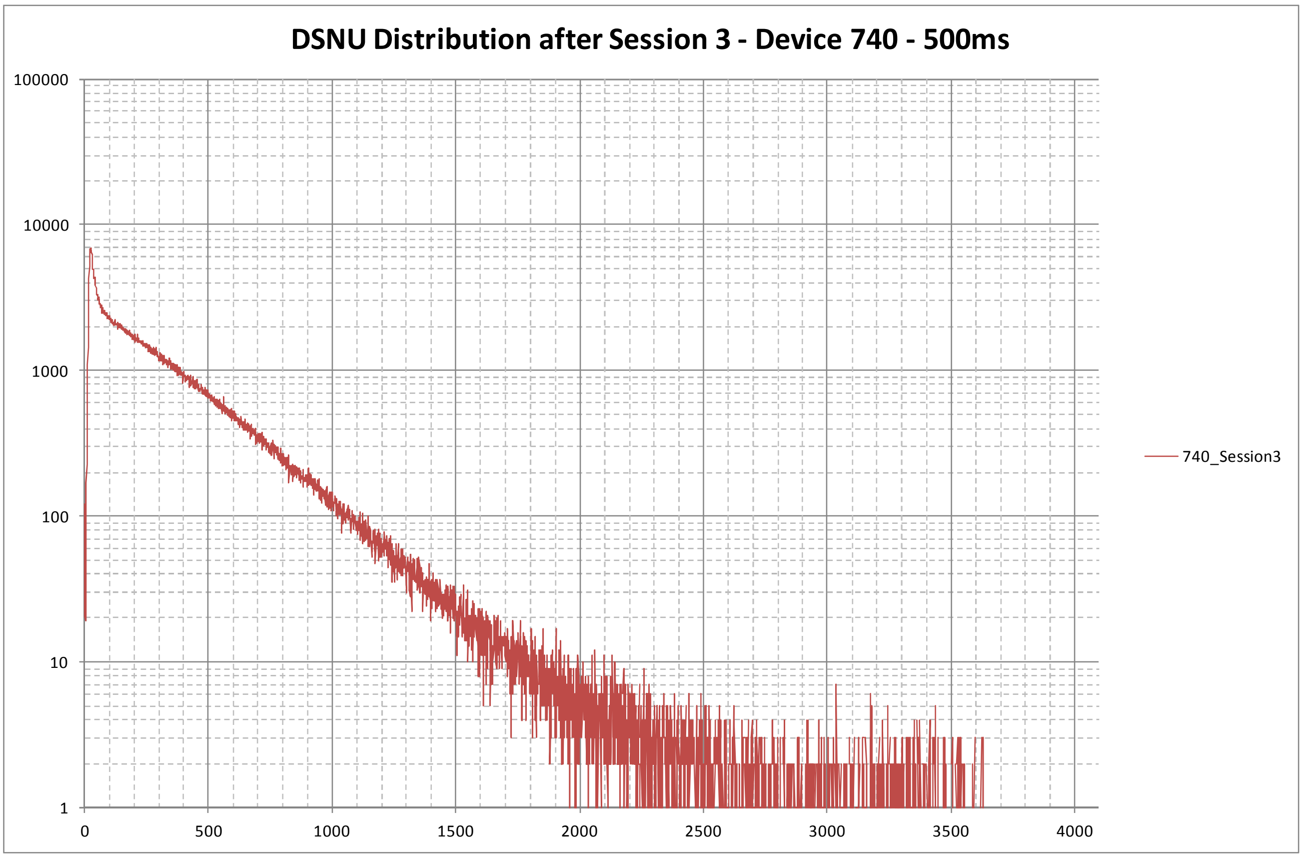

Figure 8-8: DSNU Distribution after Session 3 – Device 740 – 500ms

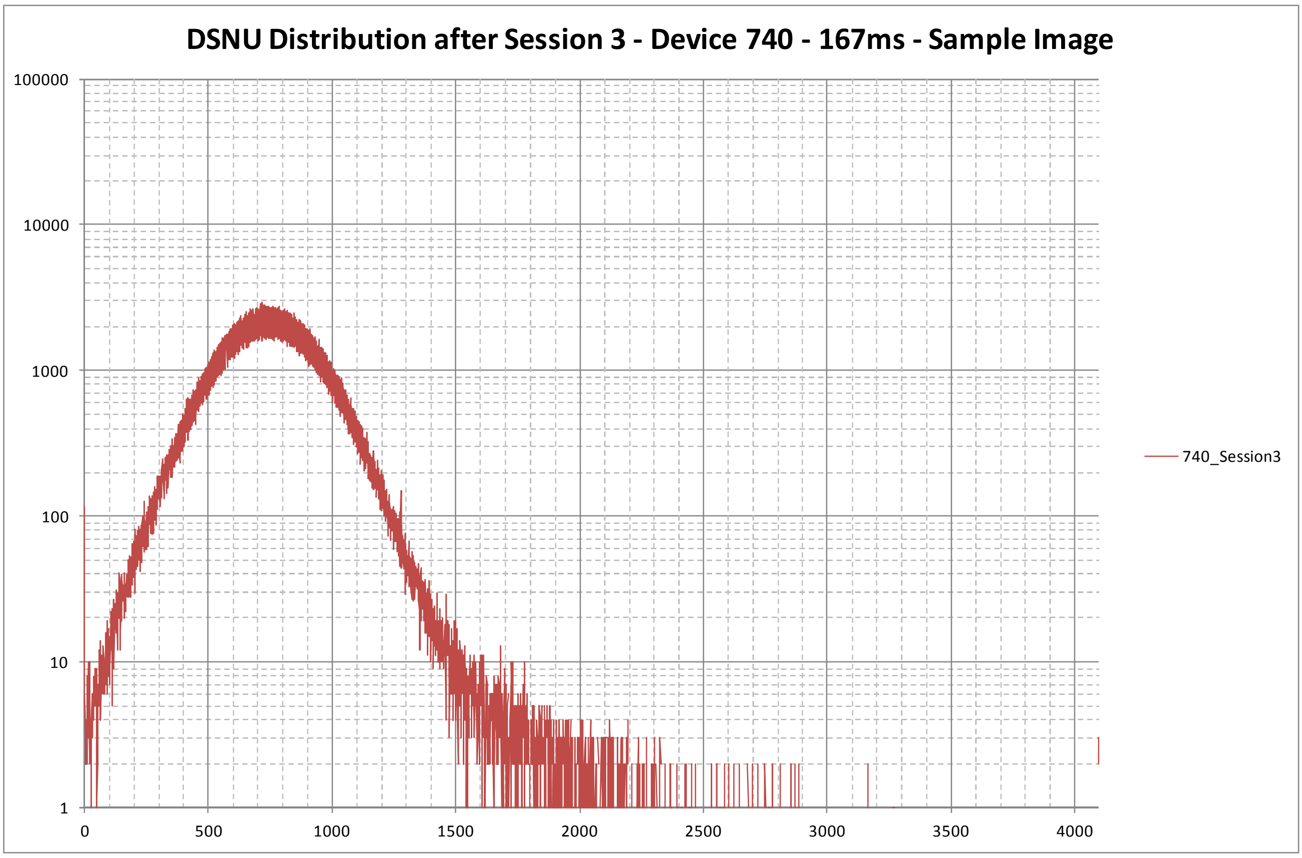

Figure 8-9 : DSNU Distribution after Session 3 – Device 740 – 167ms – Sample Image

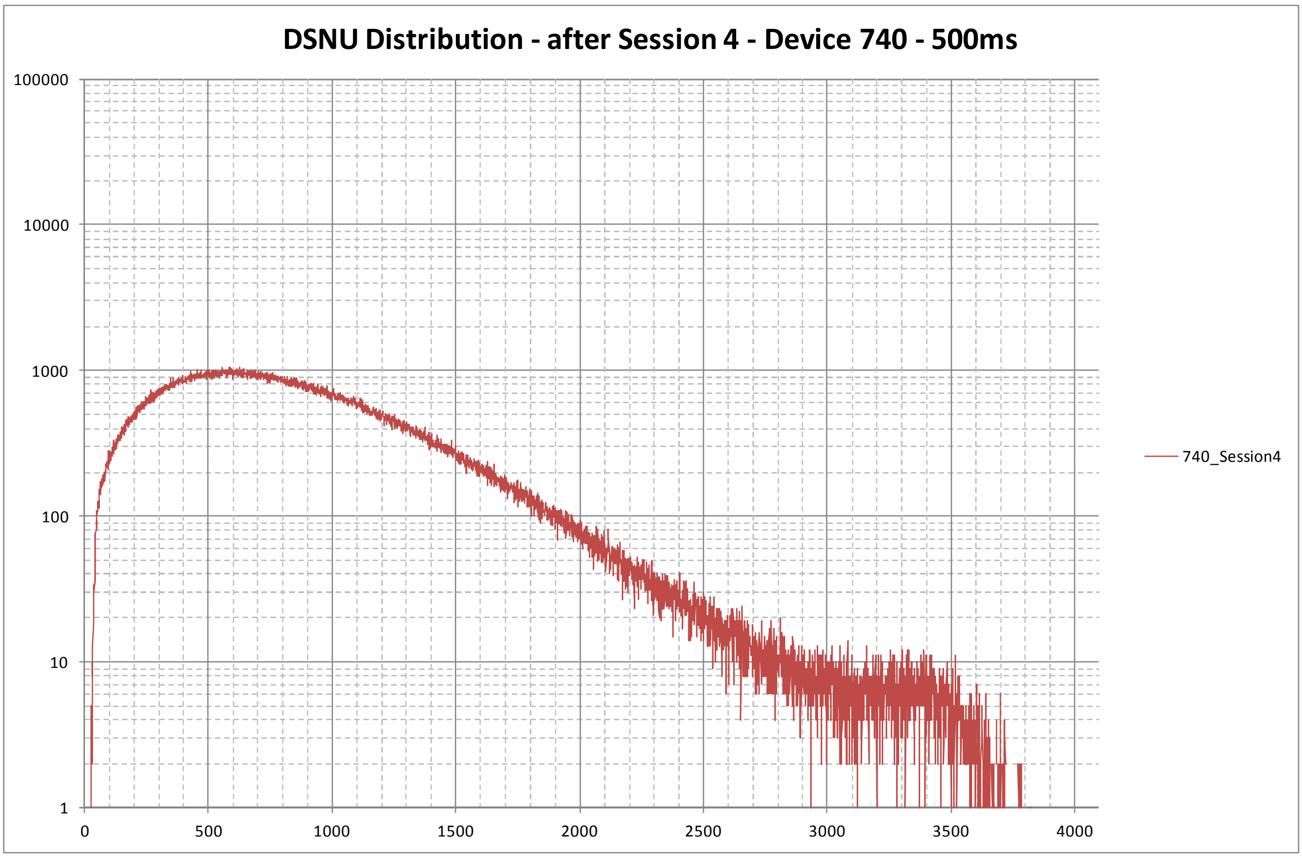

Figure 8-10: DSNU Distribution after Session 4 – Device 740 – 500ms

⇨ Some saturated pixels are visible in the histogram and will lead to a wrong interpretation of the dark current. In order to obtain the correct dark current, the dark short image is used (next page).

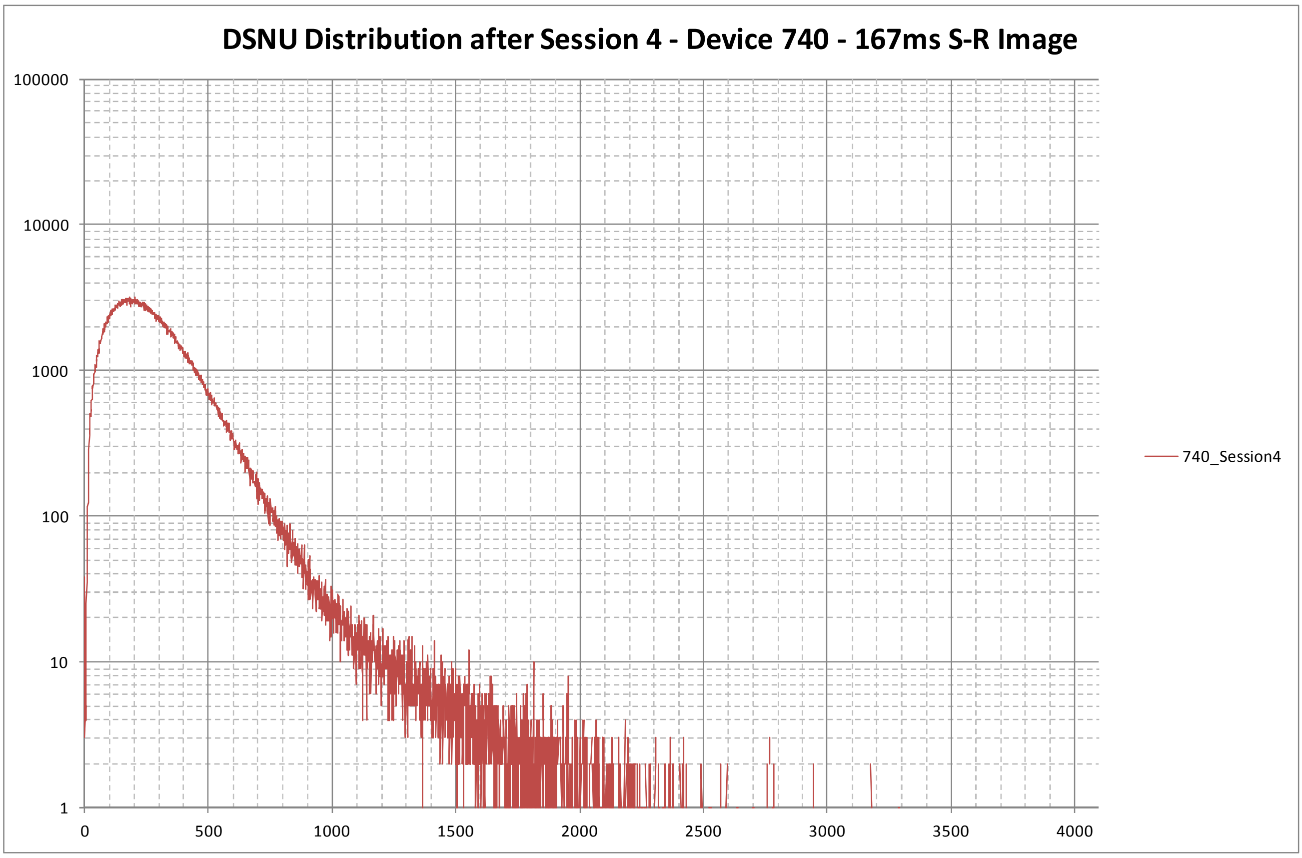

Figure 8-11: DSNU Distribution after Session 4 – Device 740 – 167ms S-R Image

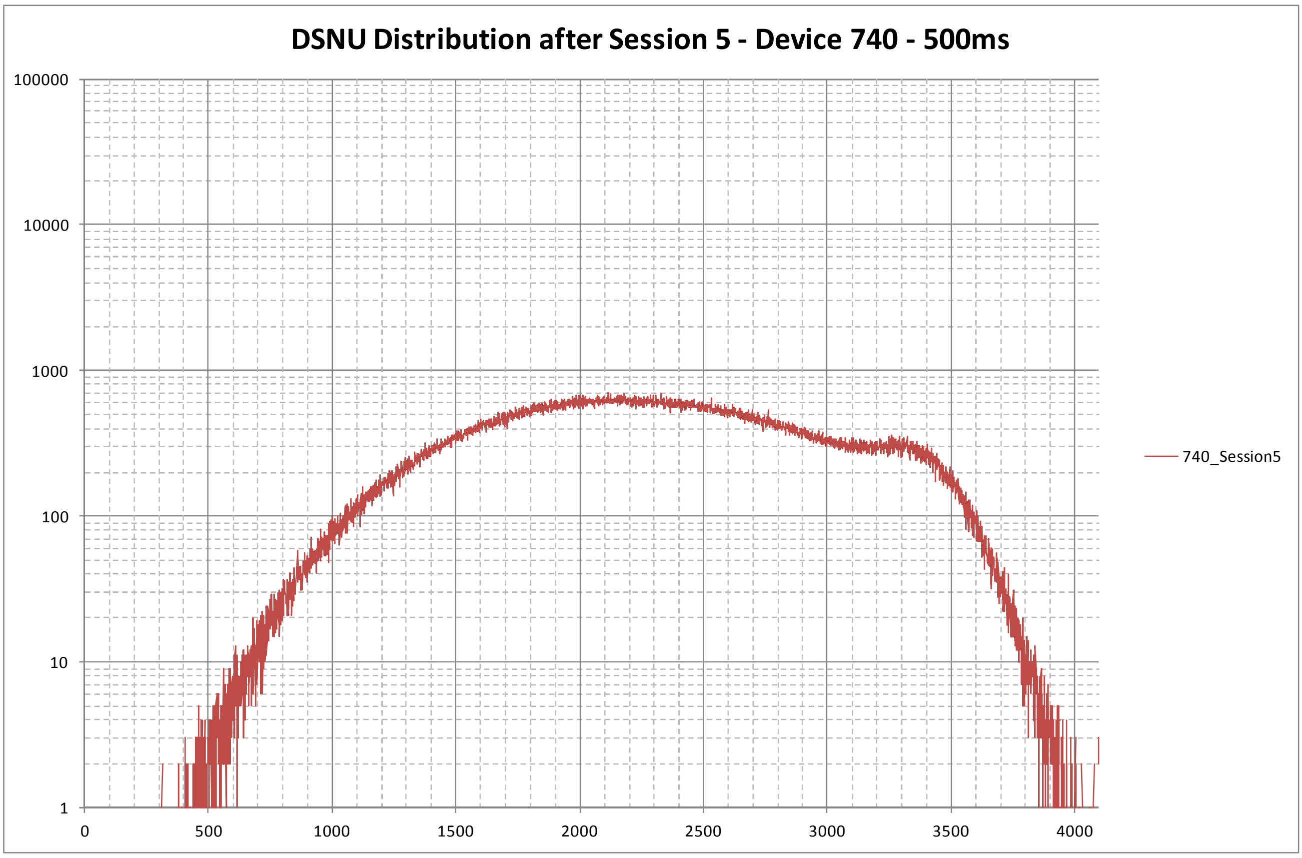

Figure 8-12 : DSNU Distribution after Session 5 – Device 740 – 500ms

⇨ Some saturated pixels are visible in the histogram and will lead to a wrong interpretation of the dark current. In order to obtain the correct dark current, the dark short image is used (next page).

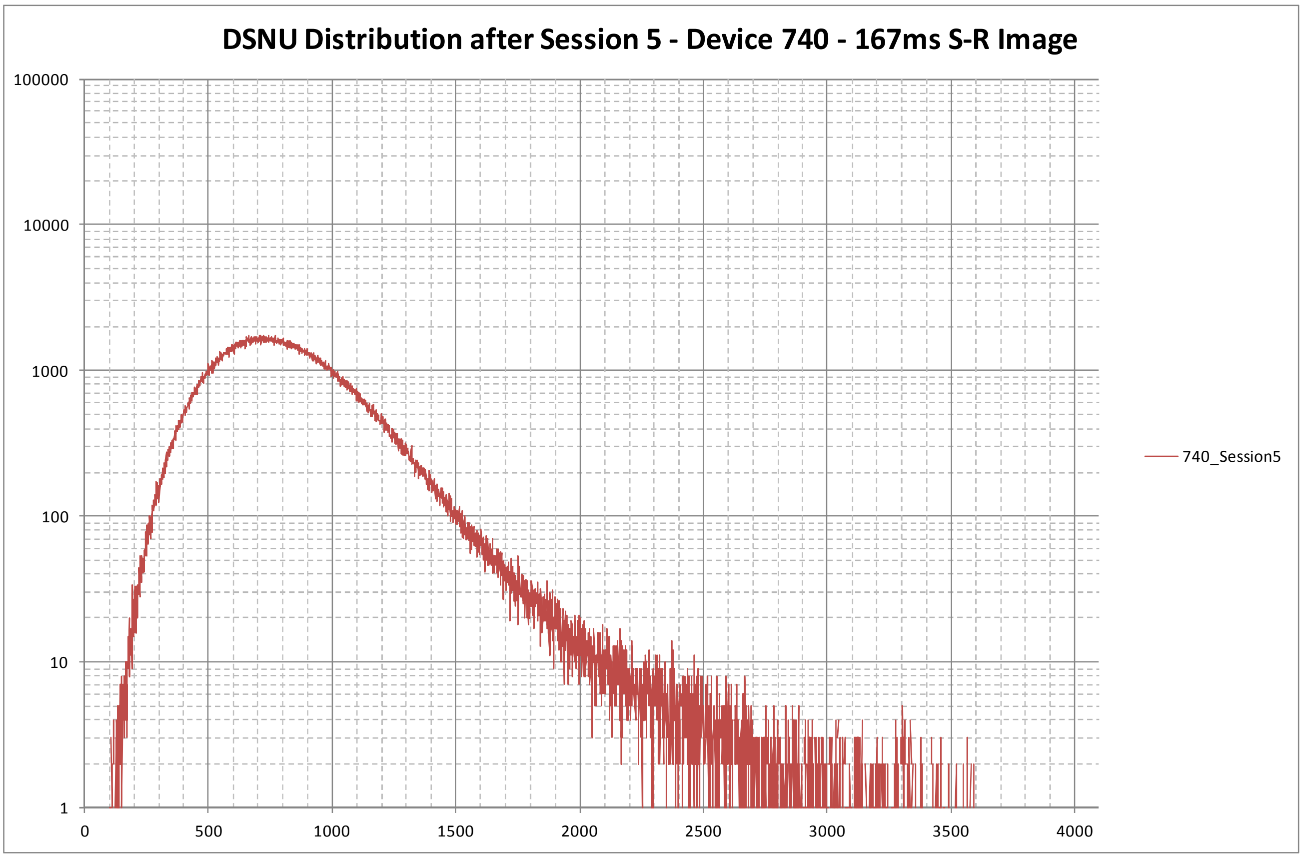

Figure 8-13 : DSNU Distribution after Session 5 – Device 740 – 167ms S-R Image

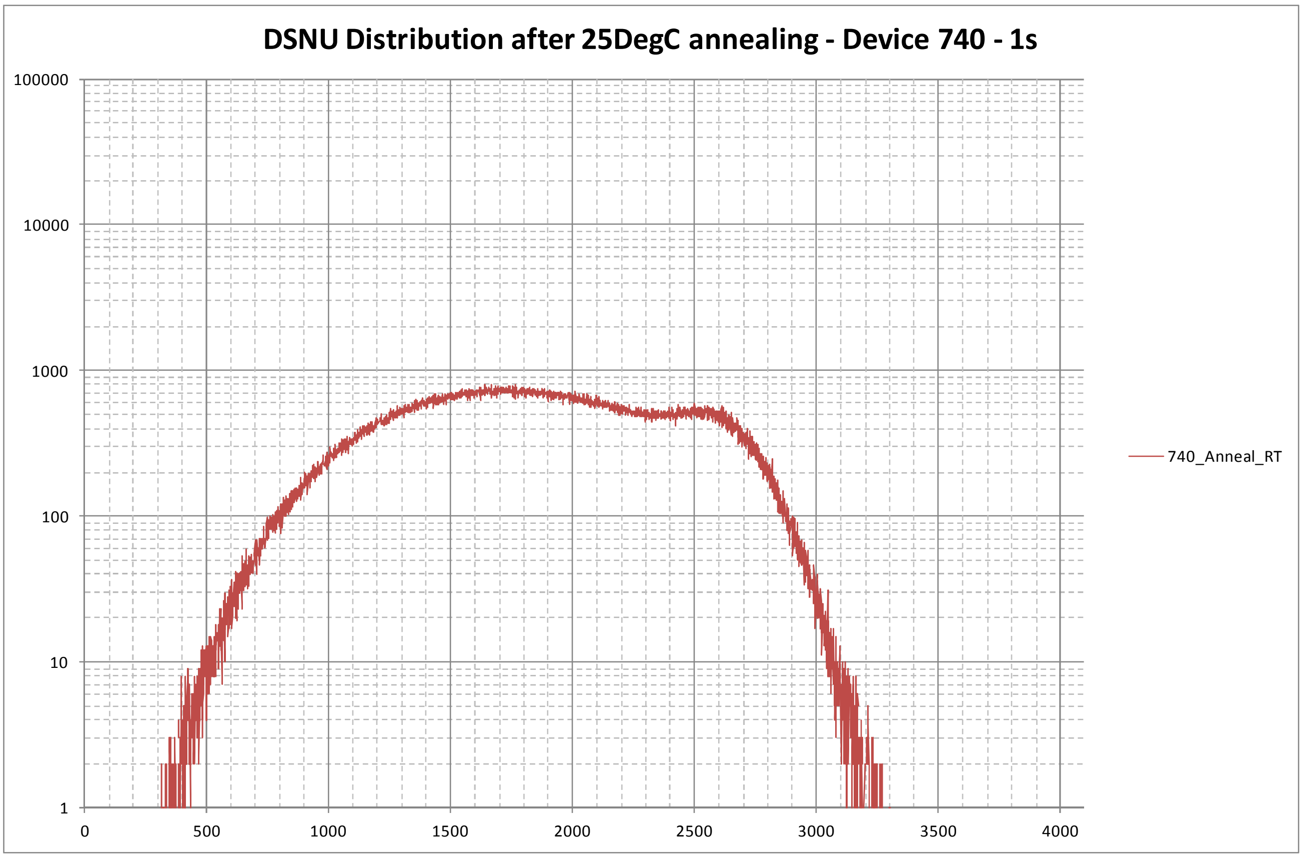

Figure 8-14 : DSNU Distribution after 25DegC annealing – Device 740 – 1s

⇨ Some saturated pixels are visible in the histogram and will lead to a wrong interpretation of the dark current. In order to obtain the correct dark current, the dark short image is used (next page).

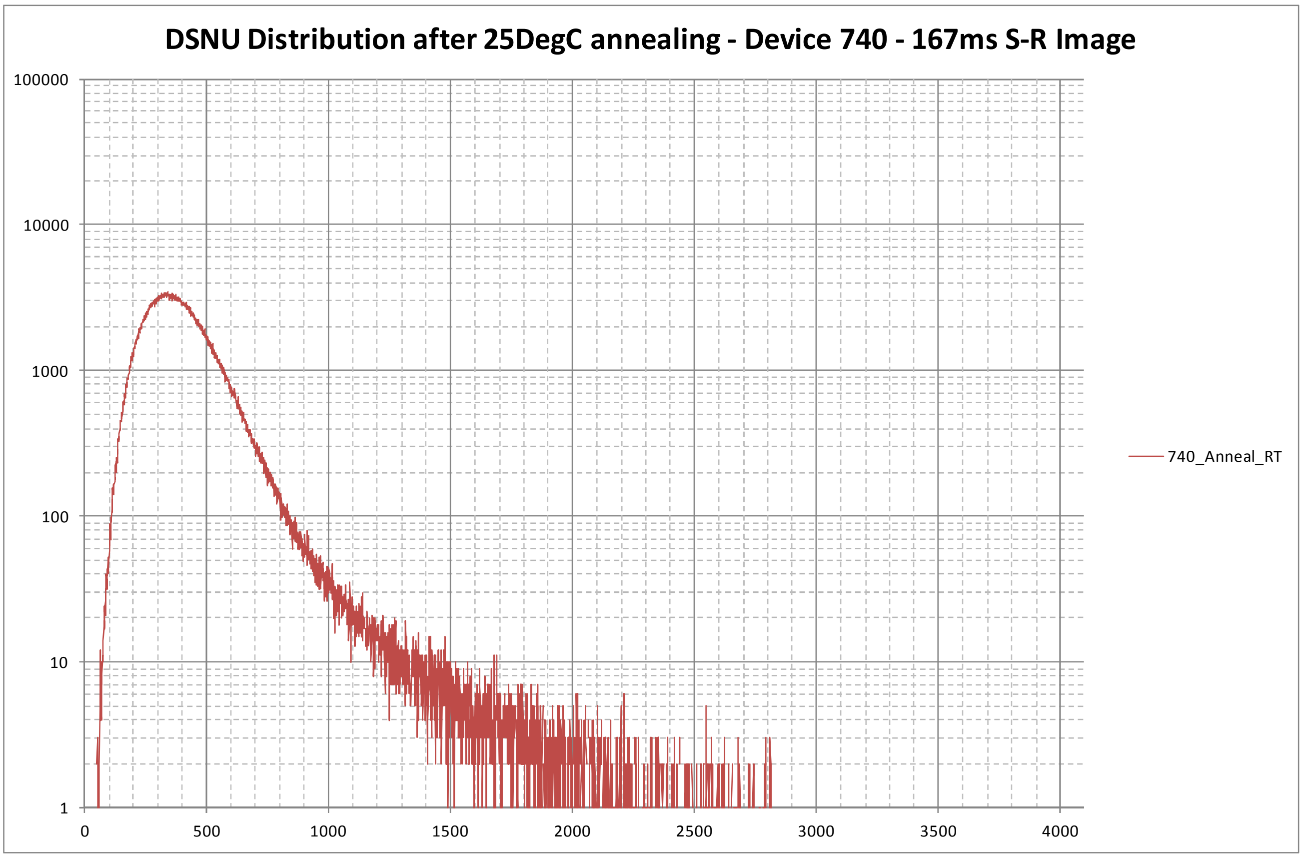

Figure 8-15 : DSNU Distribution after 25DegC annealing – Device 740 – 167ms S-R Image

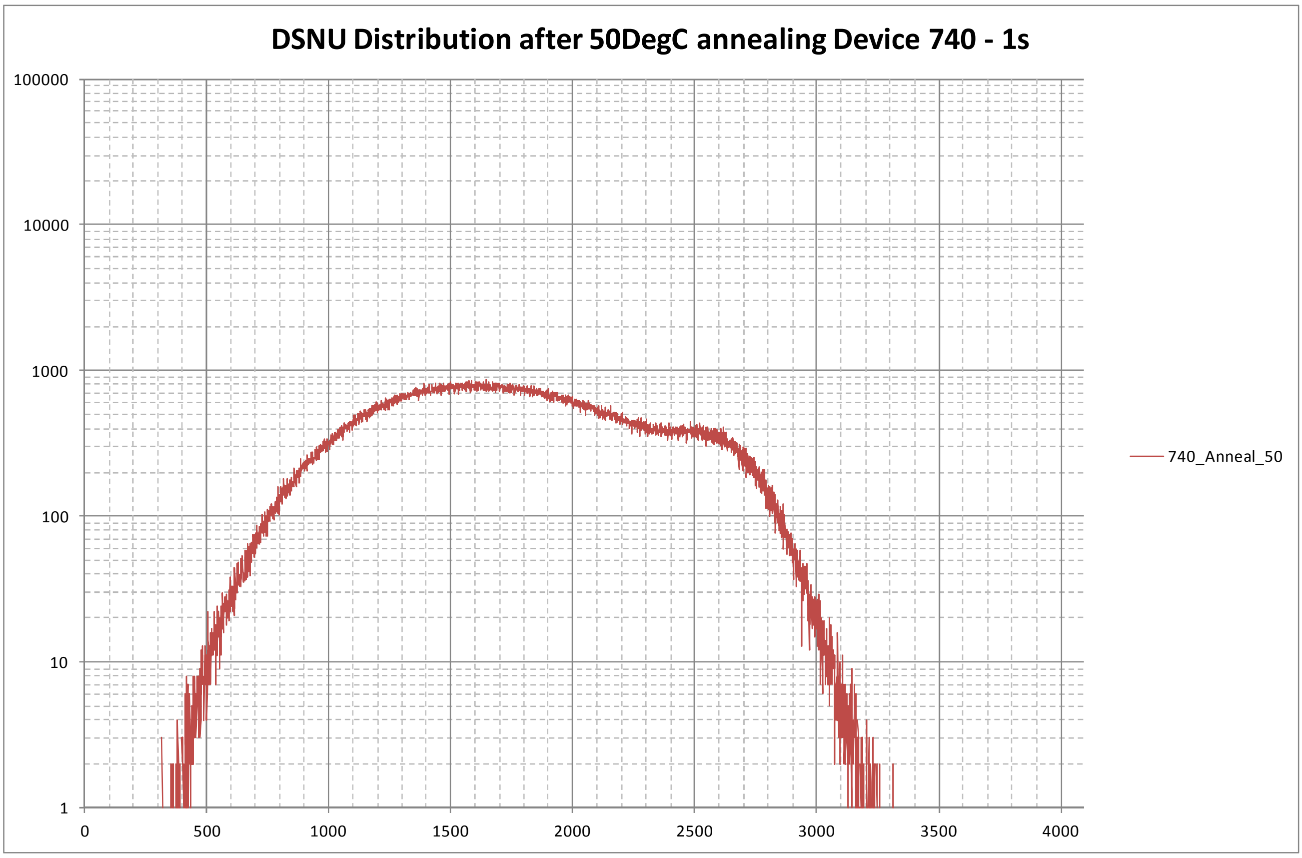

Figure 8-16 : DSNU Distribution after 50DegC annealing Device 740 – 1s

⇨ Some saturated pixels are visible in the histogram and will lead to a wrong interpretation of the dark current. In order to obtain the correct dark current, the dark short image is used (next page).

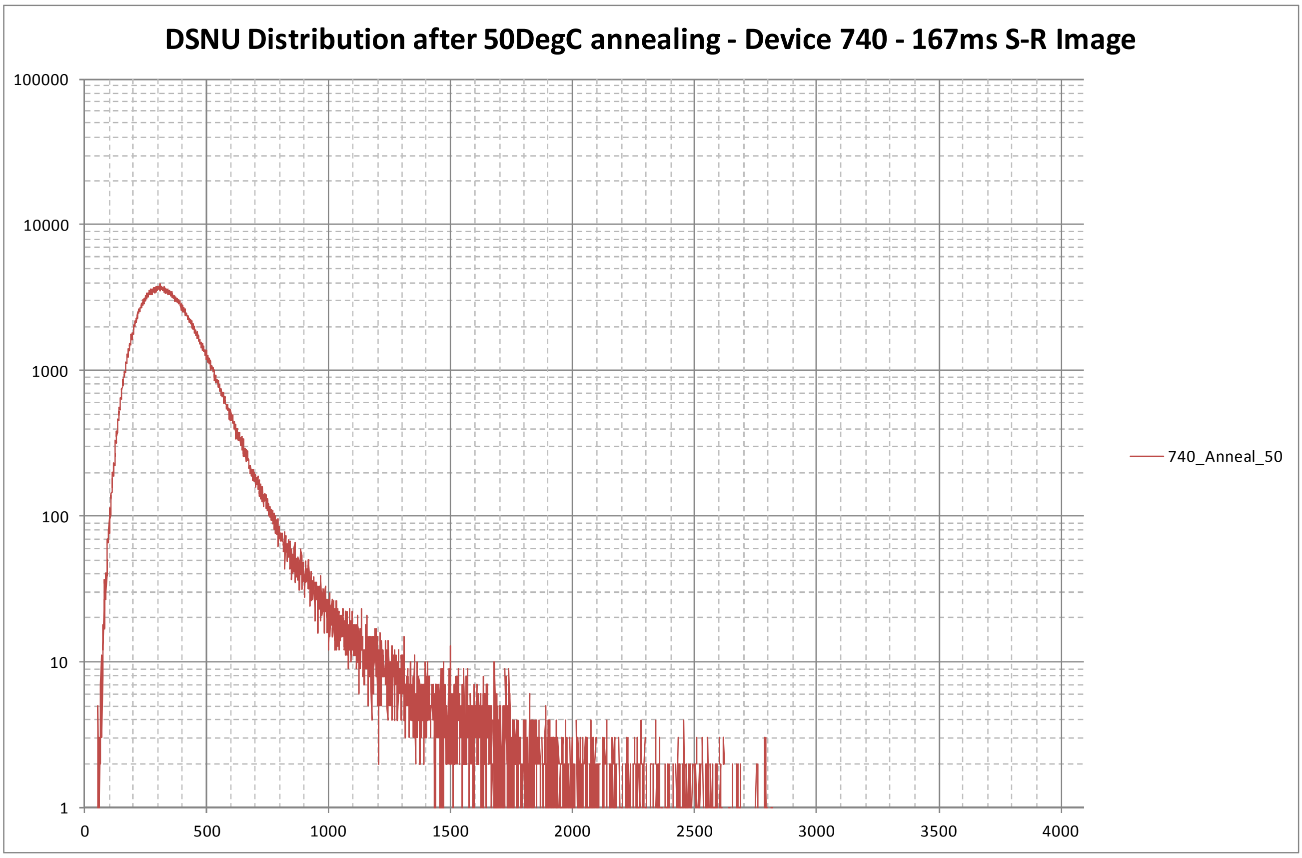

Figure 8-17 : DSNU Distribution after 50DegC annealing – Device 740 – 167ms S-R Image

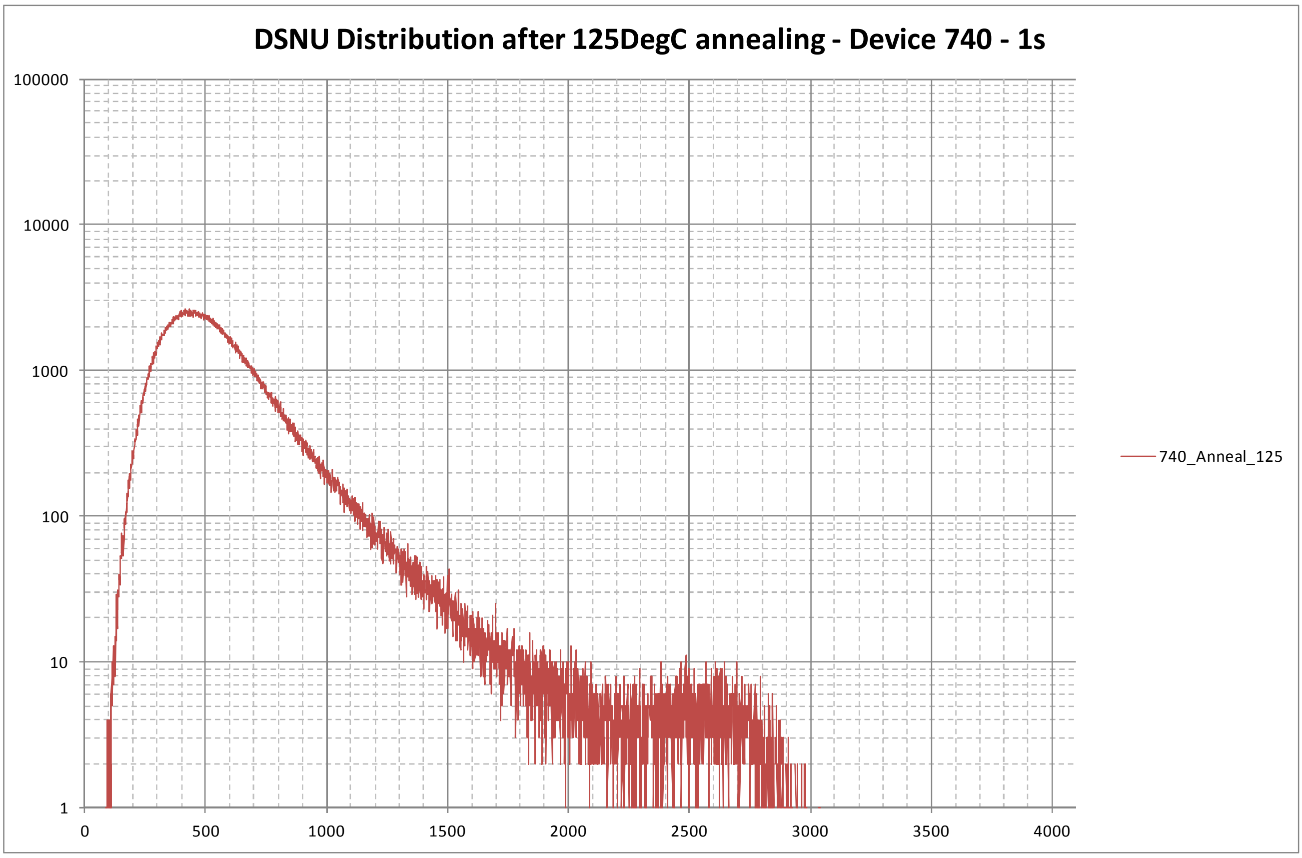

Figure 8-18 : DSNU Distribution after 125DegC annealing – Device 740 – 1s

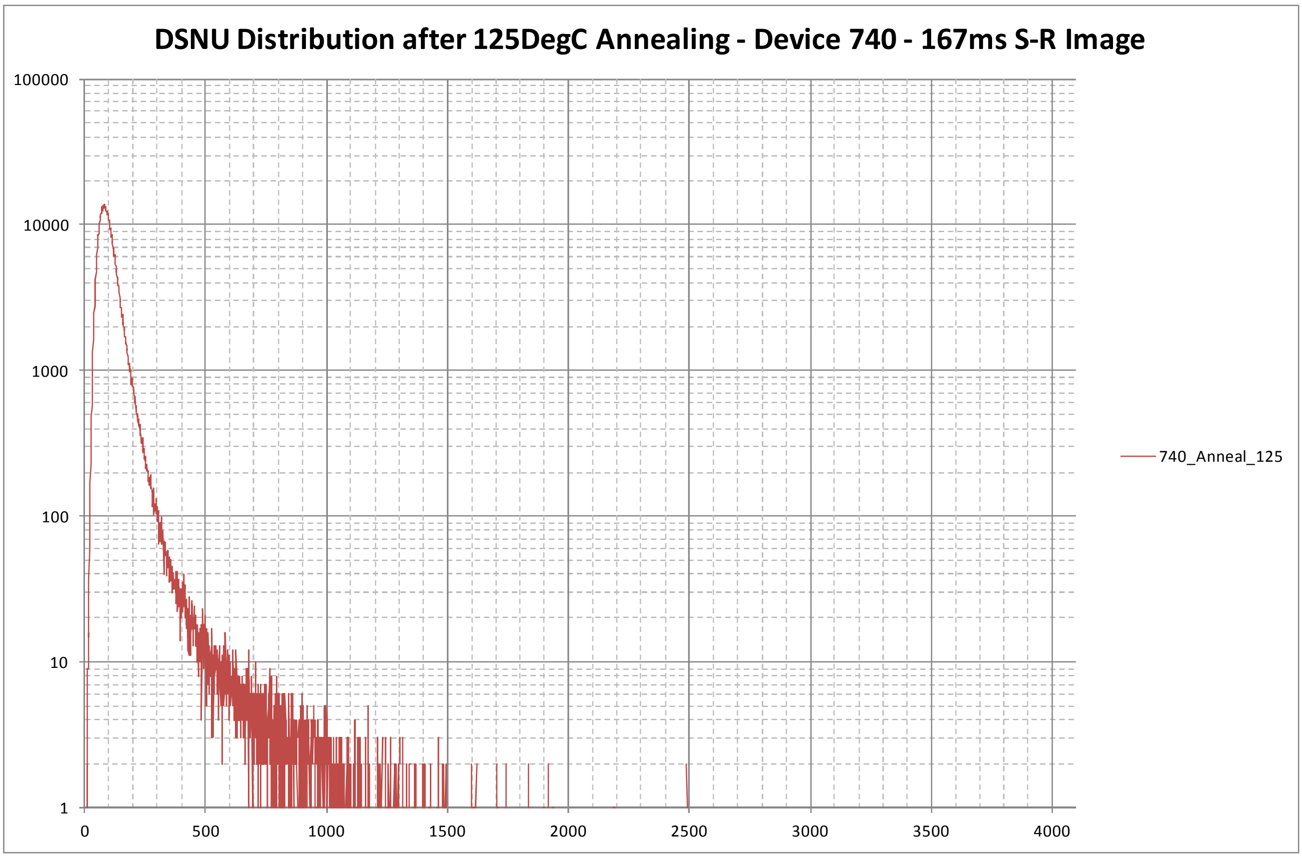

Figure 8-19 : DSNU Distribution after 125DegC Annealing – Device 740 – 167 S-R Image

8.2.2. Temporal Noise in DR Mode – hard reset

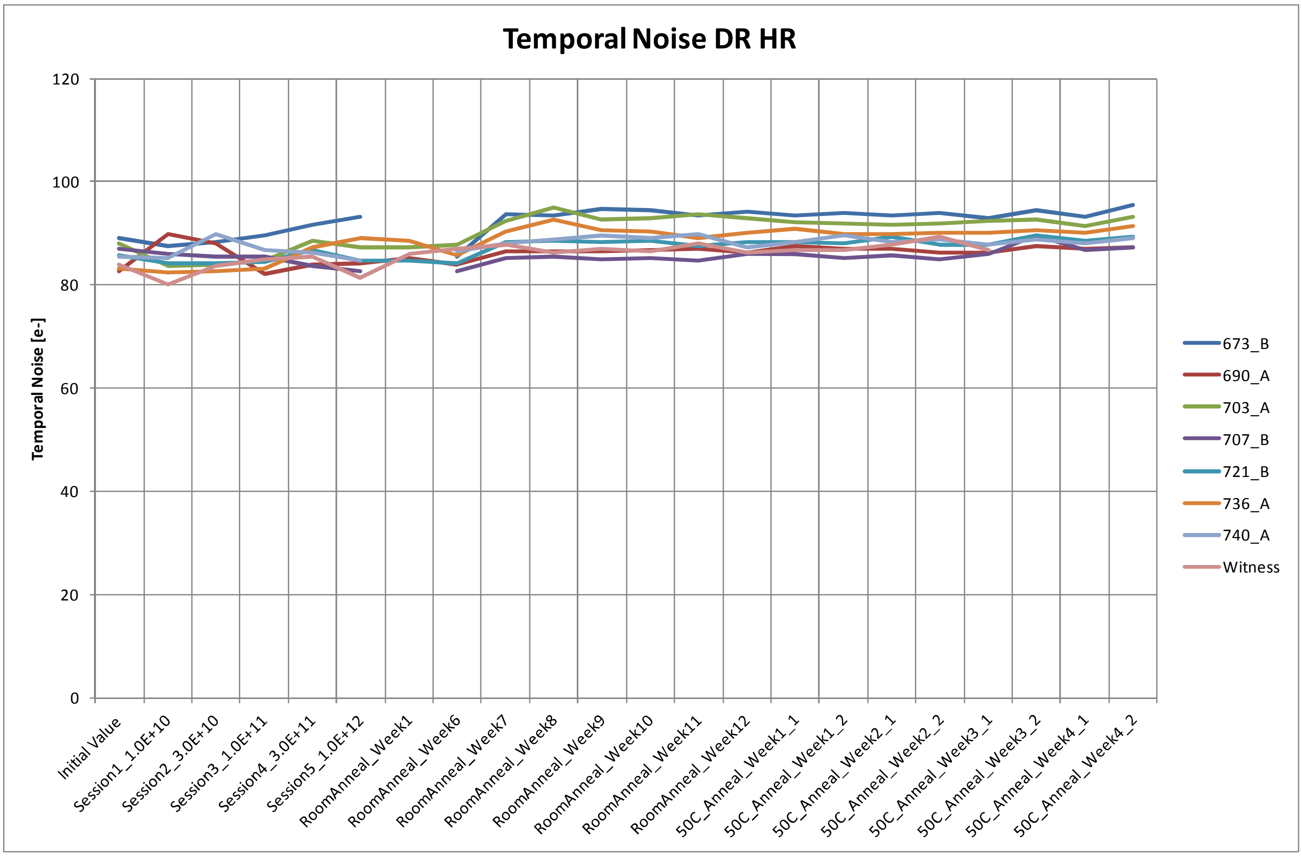

Figure 8-20: Temporal Noise in DR mode – hard reset vs radiation and annealing

The following observations are made:

- Neutron radiation has no remarkable effect on the temporal noise. The very small variations that are visible are related to test-to-test variations.
- There is no difference between the different biasing schemes.

8.2.3. Temporal Noise in DR Mode – hard to soft reset

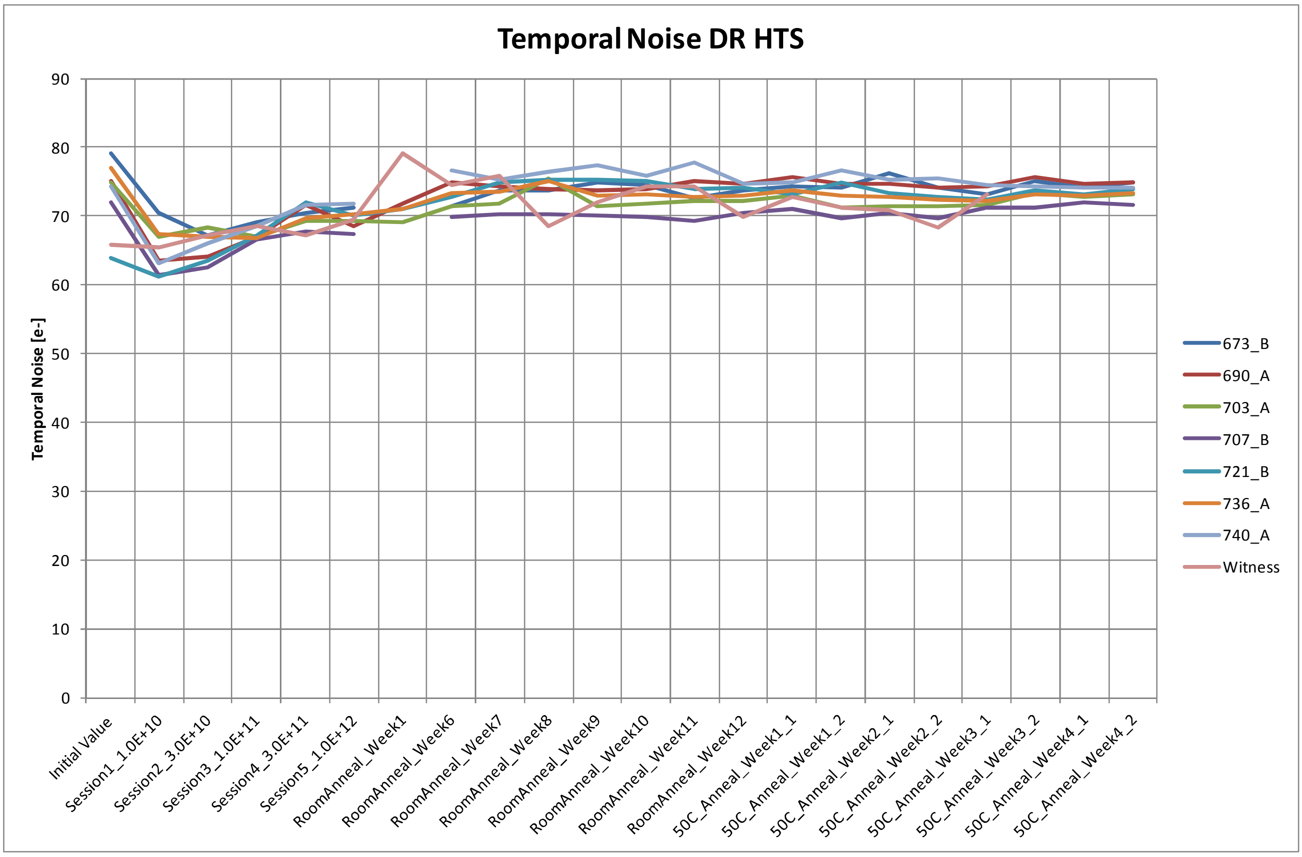

Figure 8-21: Temporal Noise in DR mode – hard to soft reset vs radiation and annealing

The following observations are made:

- Temporal noise in HTS is dropping after the first irradiation exposure to come back at its nominal values during the next irradiation exposures.

8.2.4. Temporal Noise in NDR Mode – hard reset

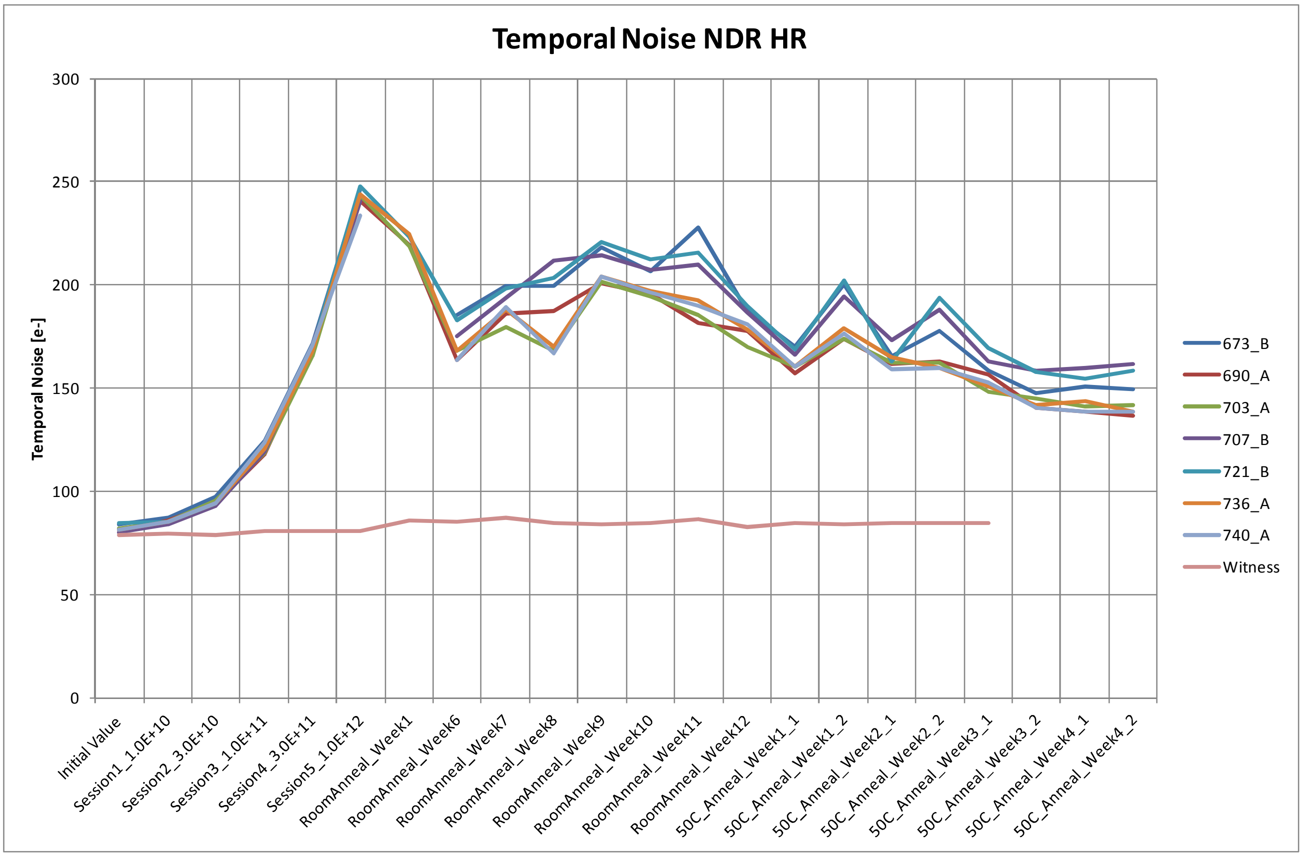

Figure 8-22: Temporal Noise in NDR mode – hard reset vs radiation and annealing

The following observations are made:

- Temporal noise is increasing with radiation. This is probably due to the 200ms minimal integration time on the tester. With increasing radiation a dark current component is added to the temporal noise. There is no difference in biasing scheme.

- Temporal noise is decreasing slightly during room temperature annealing, though the parts which were in the 'ON' state have a slightly lower temporal noise than the ones annealed in the 'OFF' state.

- Temporal noise is further decreasing during 50 degrees Celsius annealing.

8.2.5.Temporal Noise in NDR Mode – hard to soft reset

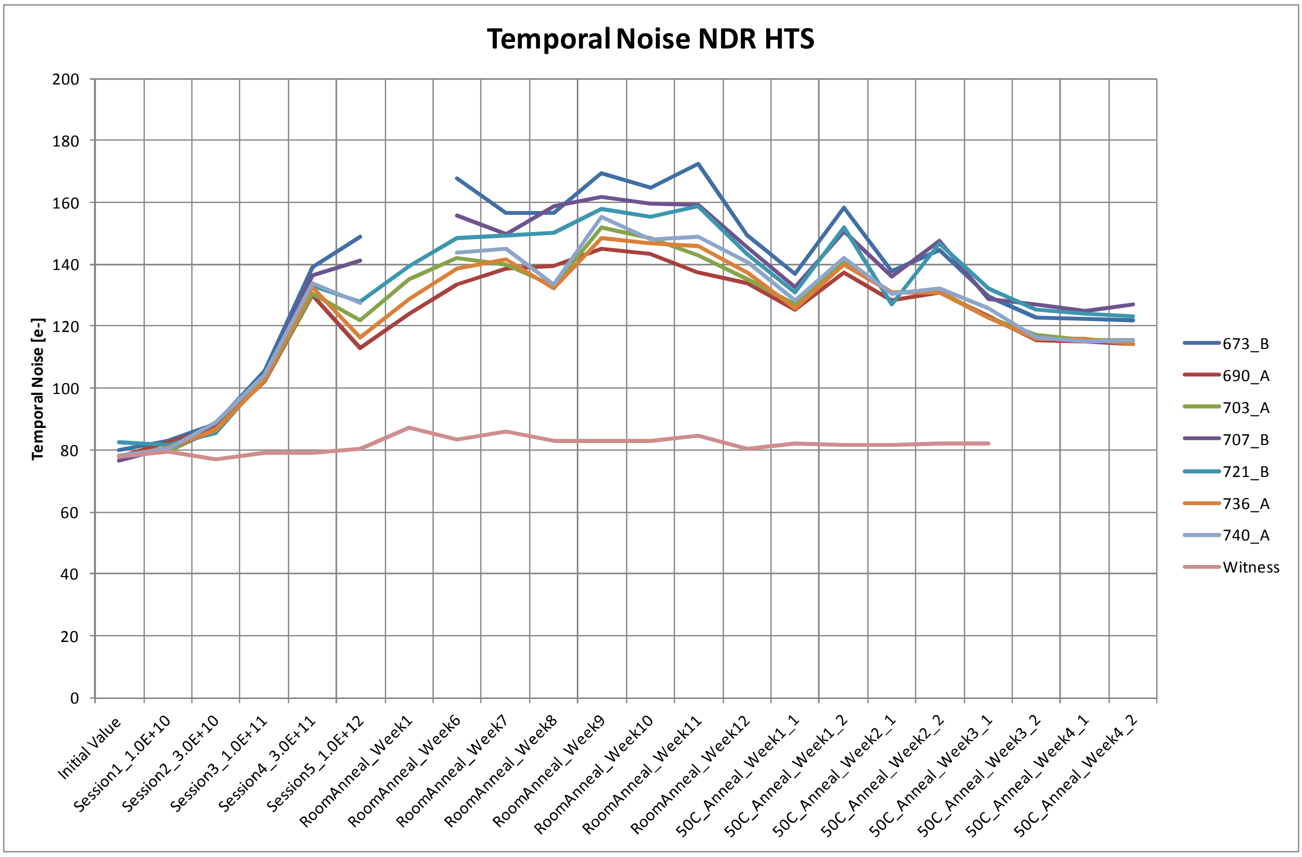

Figure 8-23: Temporal Noise in NDR mode – hard to soft reset vs radiation and annealing

The following observations are made:

- Temporal noise is increasing with radiation. This is probably due to the 200ms minimal integration time on the tester. With increasing radiation a dark current component is added to the temporal noise. There is no difference in biasing scheme.
- Temporal noise is increasing slightly during room temperature annealing. Parts annealed in the 'OFF' state have a slightly lager increase.
- Temporal noise is slightly going down during 50 degrees Celsius annealing.

8.2.6. Global Fixed Pattern Noise – hard reset

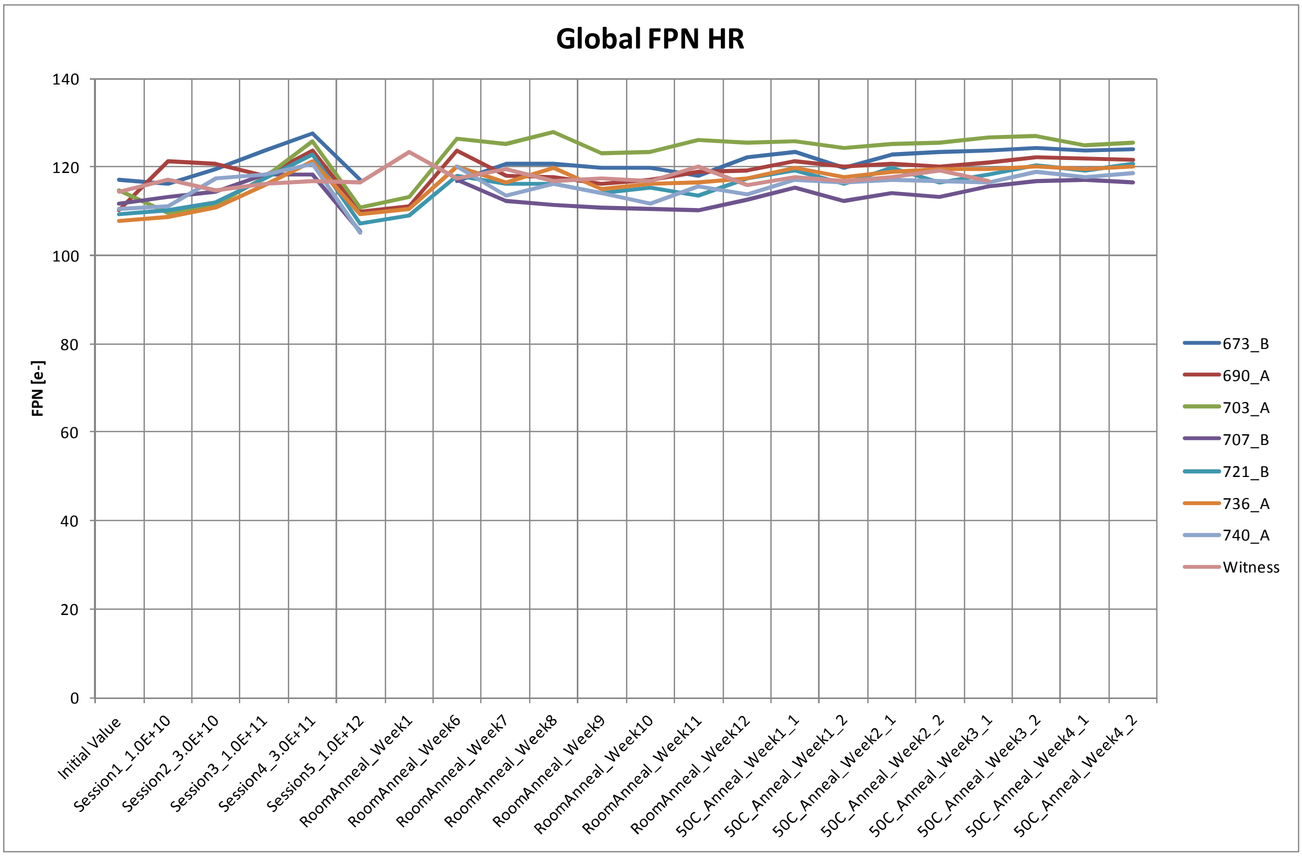

Figure 8-24: Global FPN – hard reset vs radiation and annealing

The following observations are made:

- During irradiation, FPN is slightly increasing till session 4. After session 5, FPN is back to its nominal value.
- There is no clear difference between the different biasing schemes.

8.2.7. Global Fixed Pattern Noise – hard to soft reset

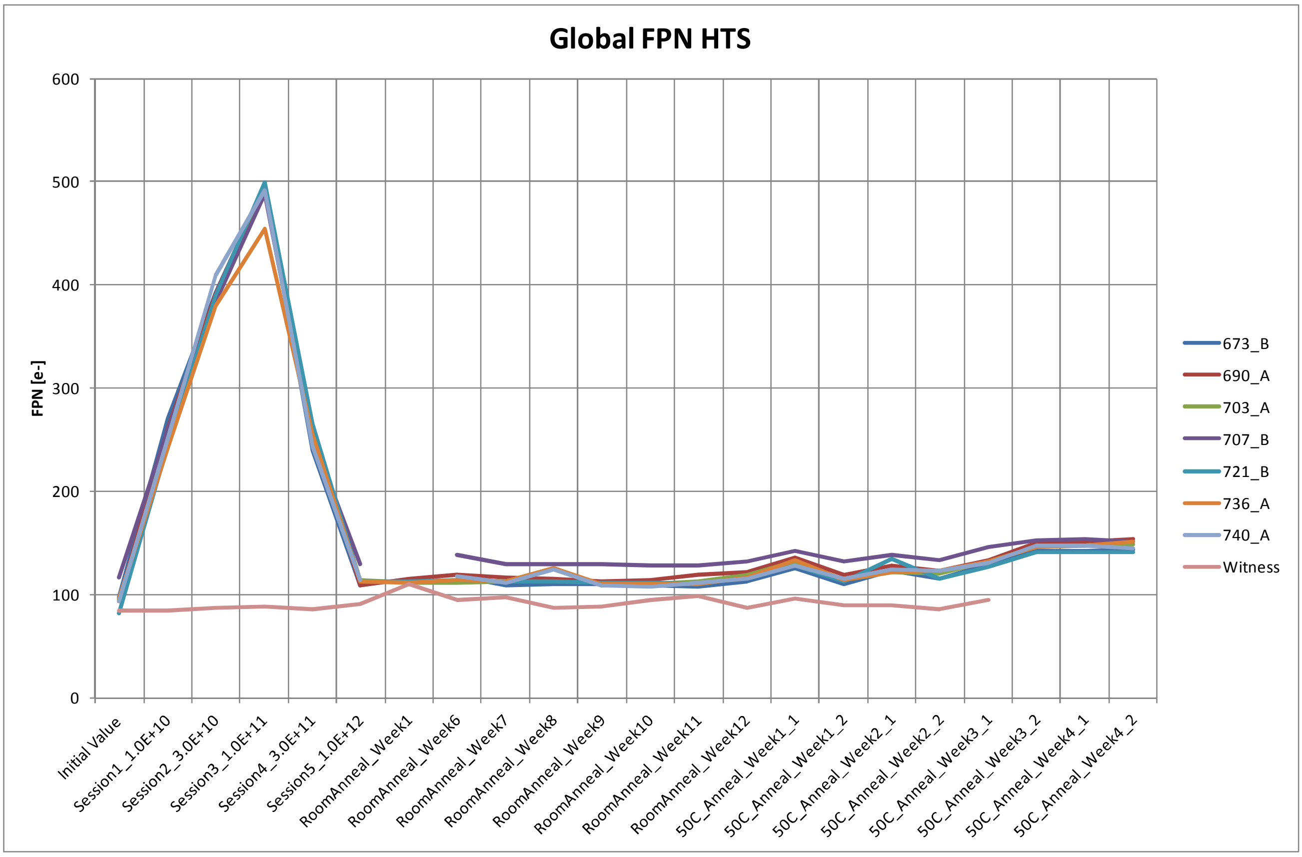

Figure 8-25 Global FPN – hard to soft reset vs radiation and annealing

The following observations are made:

- Like in the hard reset mode, FPN is increasing during the first irradiation exposures. FPN is coming back to its nominal value after the third and fourth exposure.
- FPN is slightly going up during 50 degrees Celsius annealing.
- No difference in biasing during annealing.
- The FPN increase during radiation has been verified on 3 devices that were put aside after the 3rd irradiation session. Also on those three devices the high FPN for HTS was observed. The three parts were re-measured with the new HAS tester several months after the radiation took place. The results were the same as the ones measured BOL. So probably this issue is tester related.

8.2.8. Local Fixed Pattern Noise – hard reset

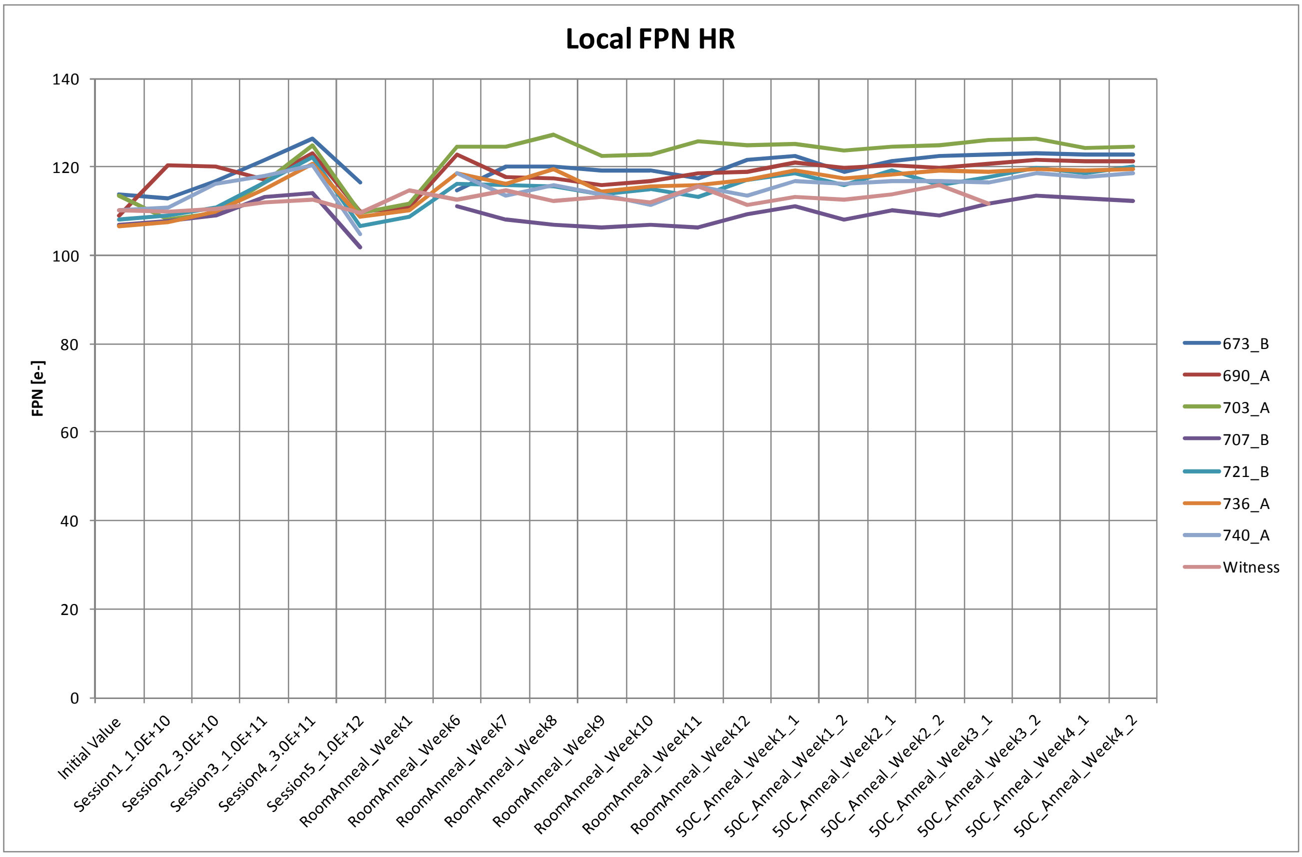

Figure 8-26 Local FPN – hard reset vs radiation and annealing

The following observations are made:

- During irradiation, FPN is slightly increasing till session 4. After session 5, FPN is back to its nominal value.
- There is no clear difference between the different biasing schemes.

8.2.9.Local Fixed Pattern Noise – hard to soft reset

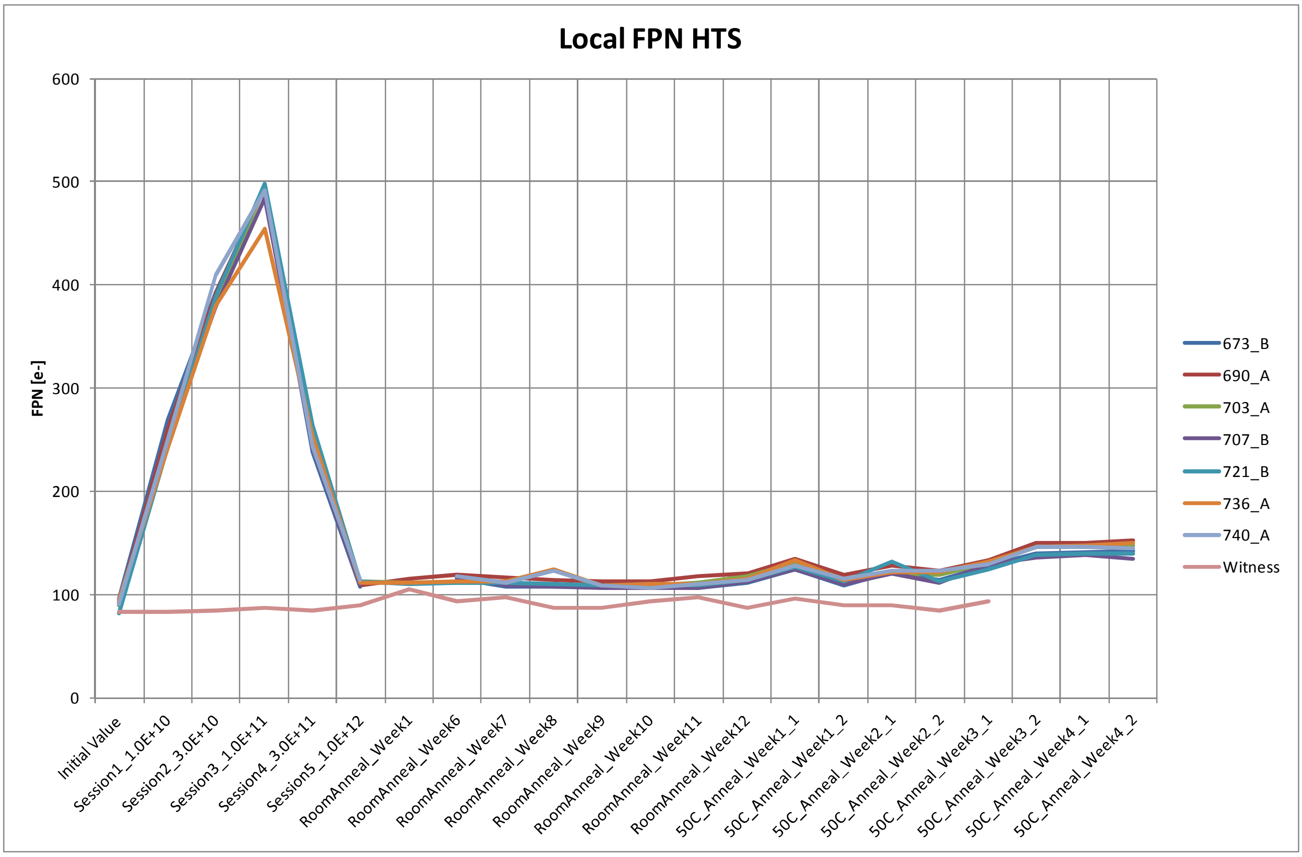

Figure 8-27: Local FPN – hard to soft reset vs radiation and annealing

The following observations are made:

- Like in the hard reset mode, FPN is increasing during the first irradiation exposures. FPN is coming back to its nominal value after the third and fourth exposure.
- FPN is slightly going up during 50 degrees Celsius annealing.
- No difference in biasing during annealing.
- The FPN increase during radiation has been verified on 3 devices that were put aside after the 3rd irradiation session. Also on those three devices the high FPN for HTS was observed. The three parts were re-measured with the new HAS tester several months after the radiation took place. The results were the same as the ones measured BOL. So probably this issue is tester related.

8.2.10.Global Photo Response Non Uniformity

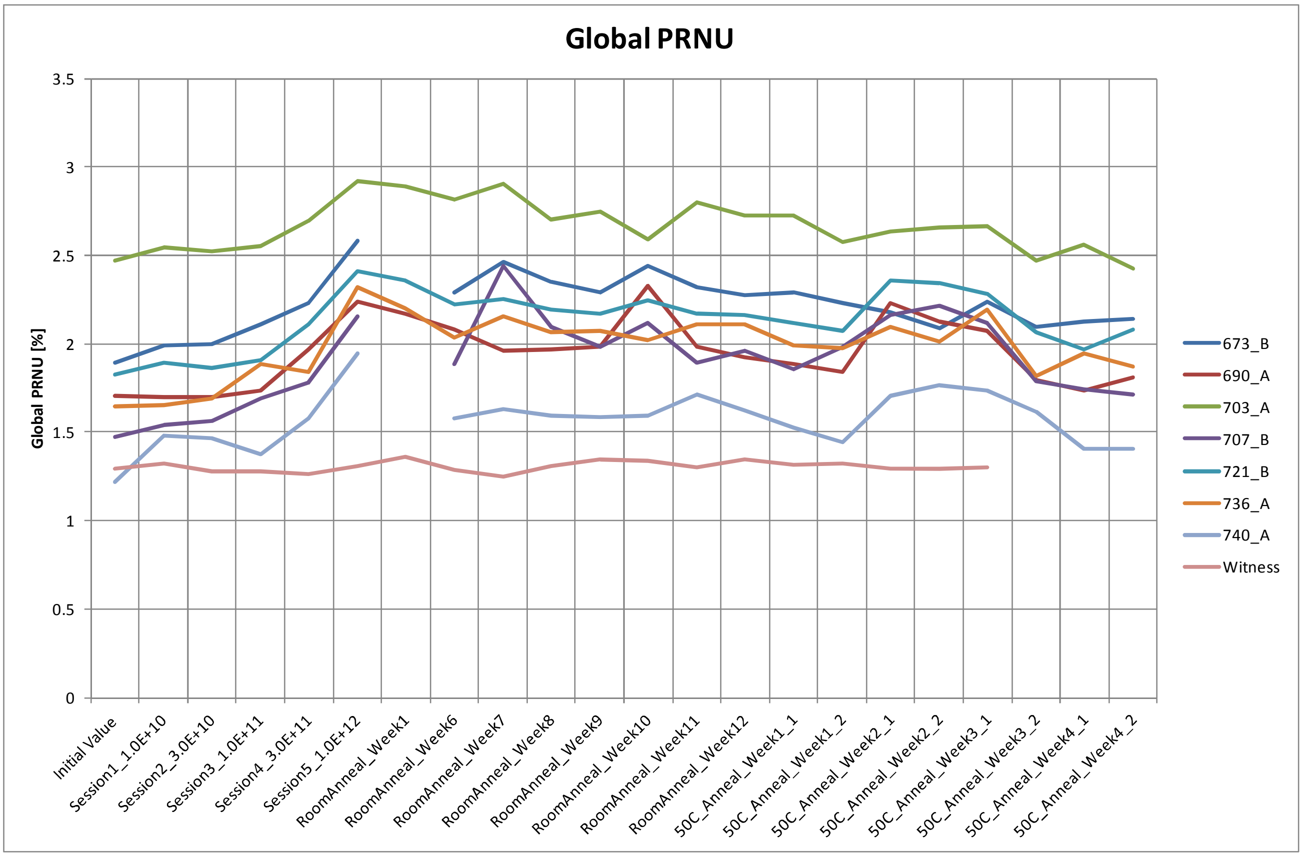

Figure 8-28: Global PRNU vs radiation and annealing

The following observations are made:

- According to the above graph, PRNU is increasing with radiation. This is a wrong interpretation as PRNU is increasing due to the sensitivity which is going down with increased radiation. PRNU is expressed as (standard deviation / average grey value). If the average grey value goes down, the PRNU goes up.
- PRNU is slightly moving back to its initial value during room temperature and 50 degrees Celsius annealing.
- No difference in biasing during annealing.

8.2.11. Local Photo Response Non Uniformity

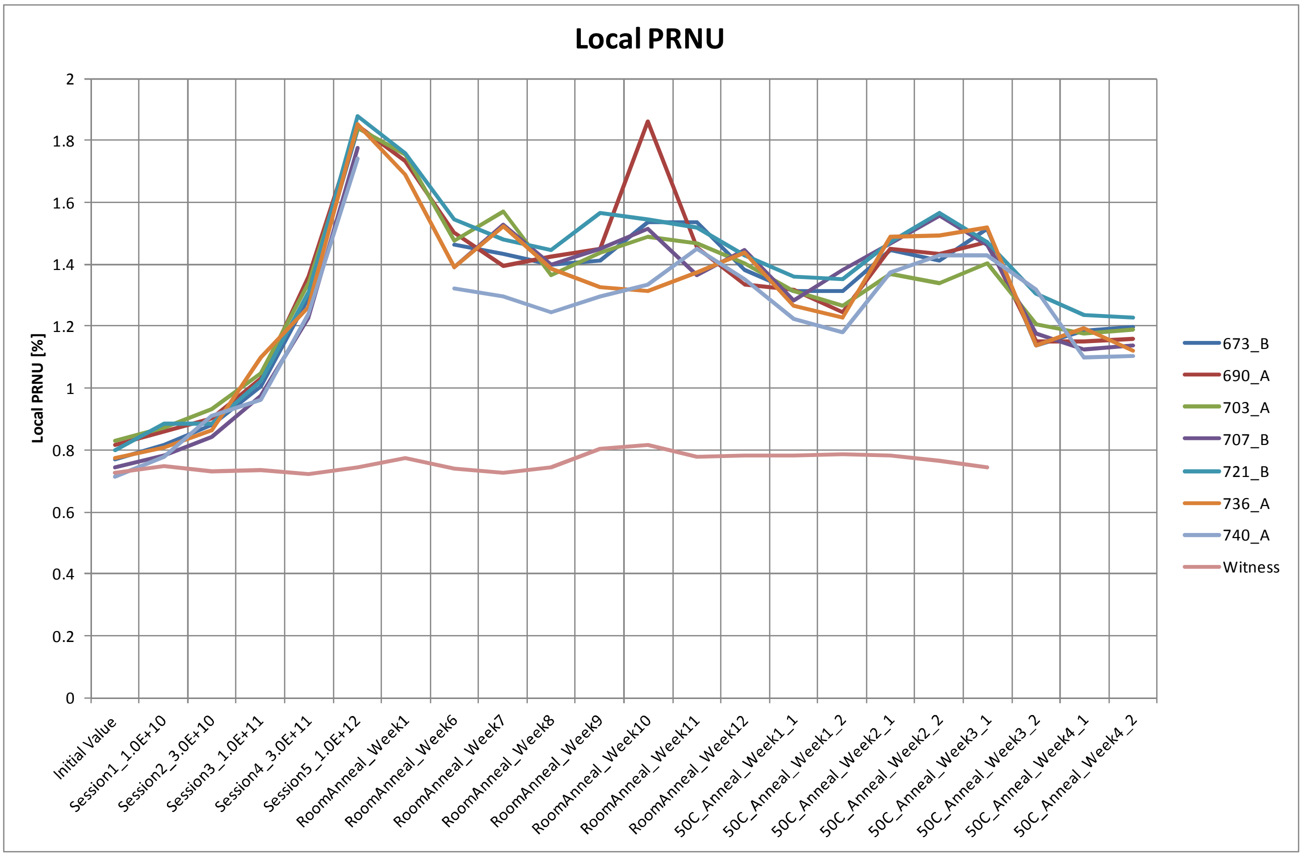

Figure 8-29: Local PRNU vs radiation and annealing

The following observations are made:

- According to the above graph, PRNU is increasing with radiation. This is a wrong interpretation as PRNU is increasing due to the sensitivity which is going down with increased radiation. PRNU is expressed as (standard deviation / average grey value). If the average grey value goes down, the PRNU goes up.
- PRNU is slightly moving back to its initial value during room temperature and 50 degrees Celsius annealing.
- No difference in biasing during annealing.

8.2.12.Operating Current

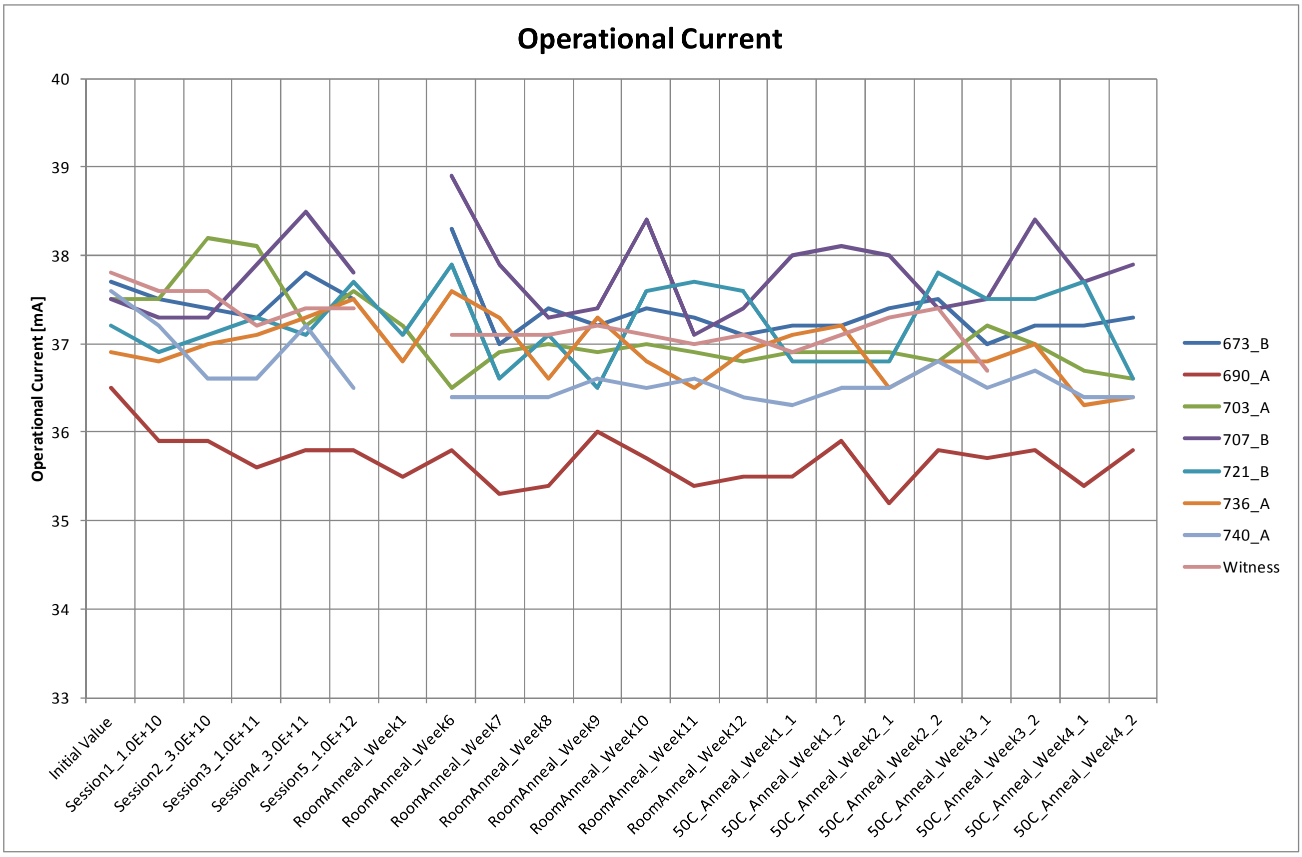

Figure 8-30: Operating Current vs radiation and annealing

The following observations are made:

- The operation current does not change over radiation, room temperature annealing and 50 degrees Celsius annealing. Also the different biasing schemes have no influence.

8.2.13. Standby Current

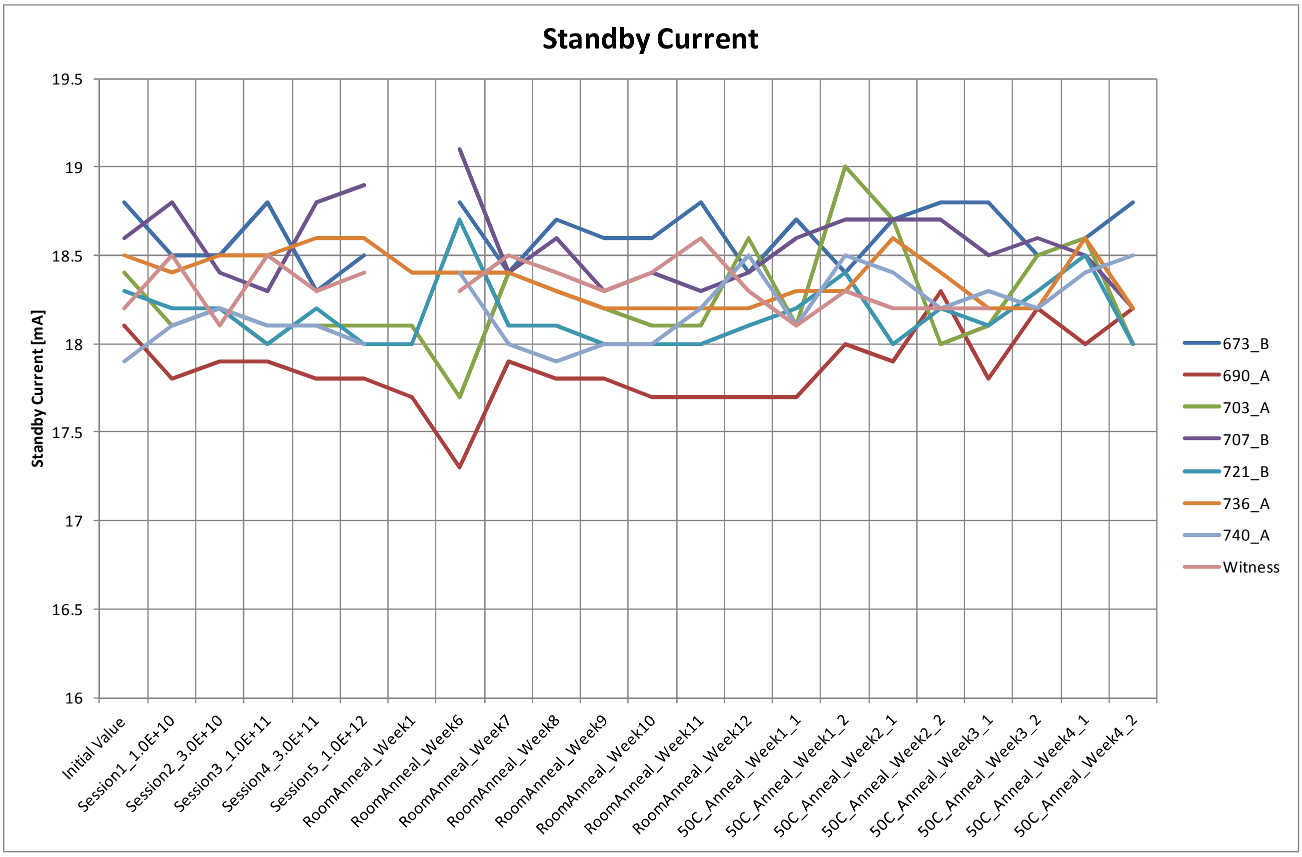

Figure 8-31: Standby Current vs radiation and annealing

The following observations are made:

- The standby current does not change over radiation, room temperature annealing and 50 degrees Celsius annealing. Also the different biasing schemes have no influence.

8.2.14. DSNU

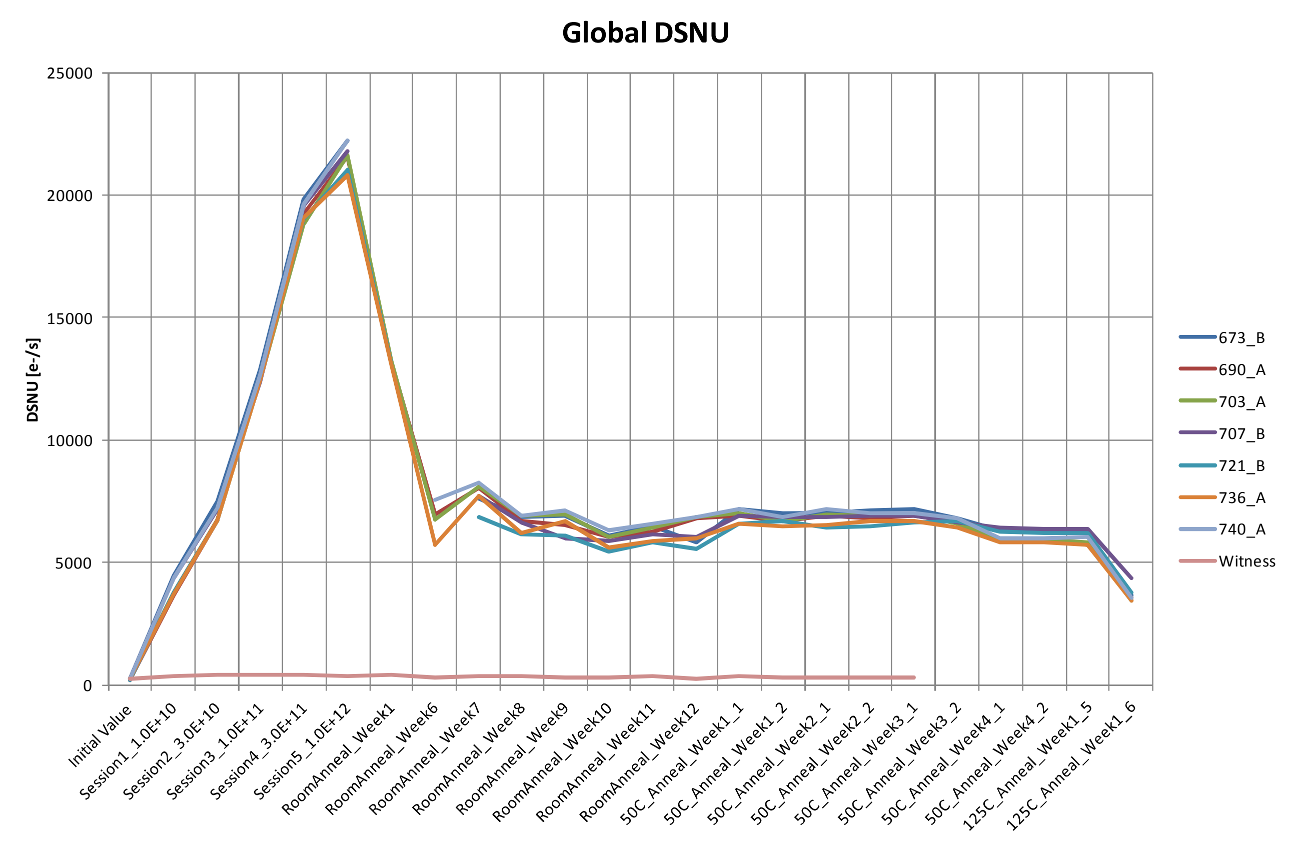

Figure 8-32: DSNU vs radiation and annealing

The following observations are made:

- Like the dark current, DSNU is increasing during the consecutive irradiation exposures.
- DSNU is dropping fast during room temperature annealing.
- DSNU does not significantly change during 50 degrees Celsius annealing.
- DSNU is dropping after 125 degrees Celsius annealing.
- No difference in biasing during annealing.

8.2.15.INL

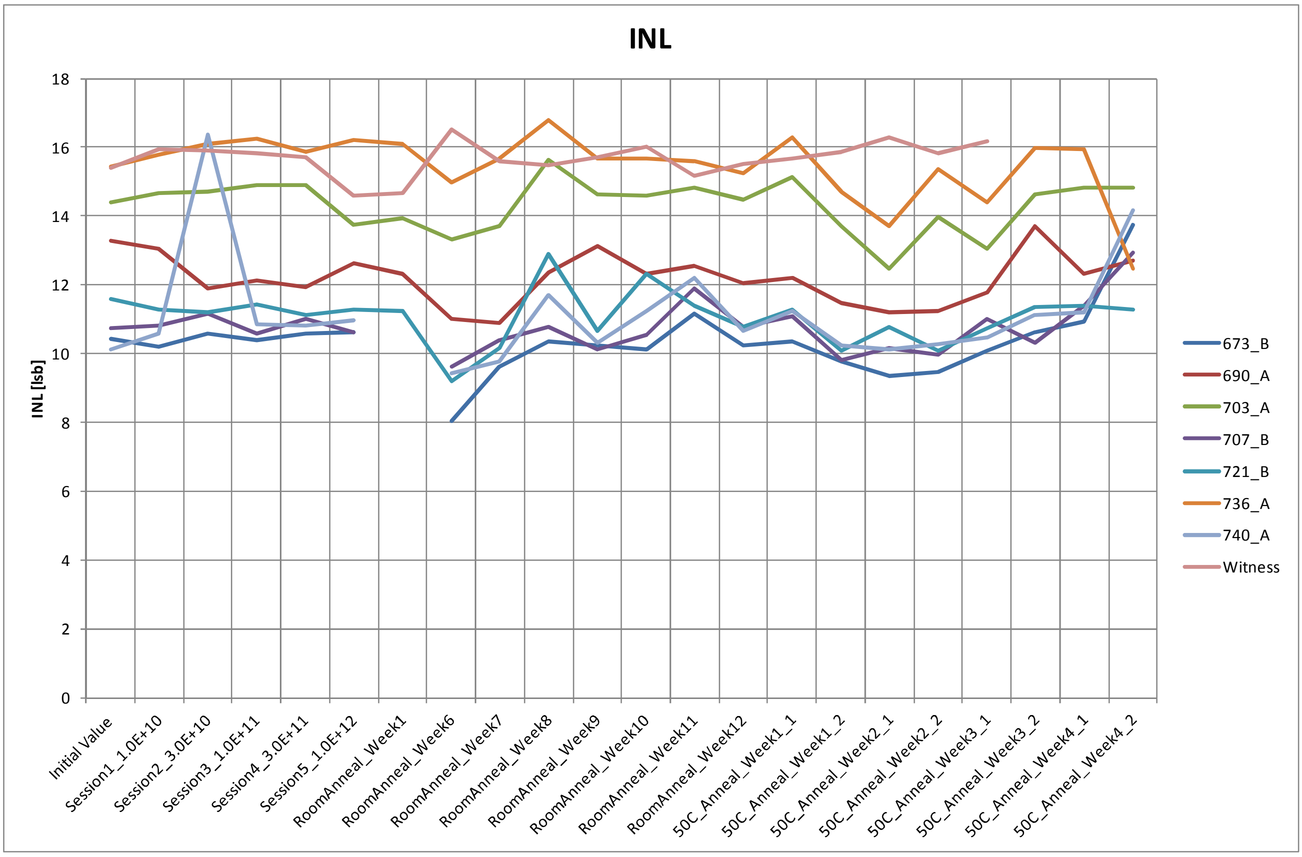

Figure 8-33: INL vs radiation and annealing

The following observations are made:

- INL is a very unstable measurement due to the behavior of the HAS2 ADC.
- There’s no increase or decrease visible during radiation or annealing.

8.2.16.DNL

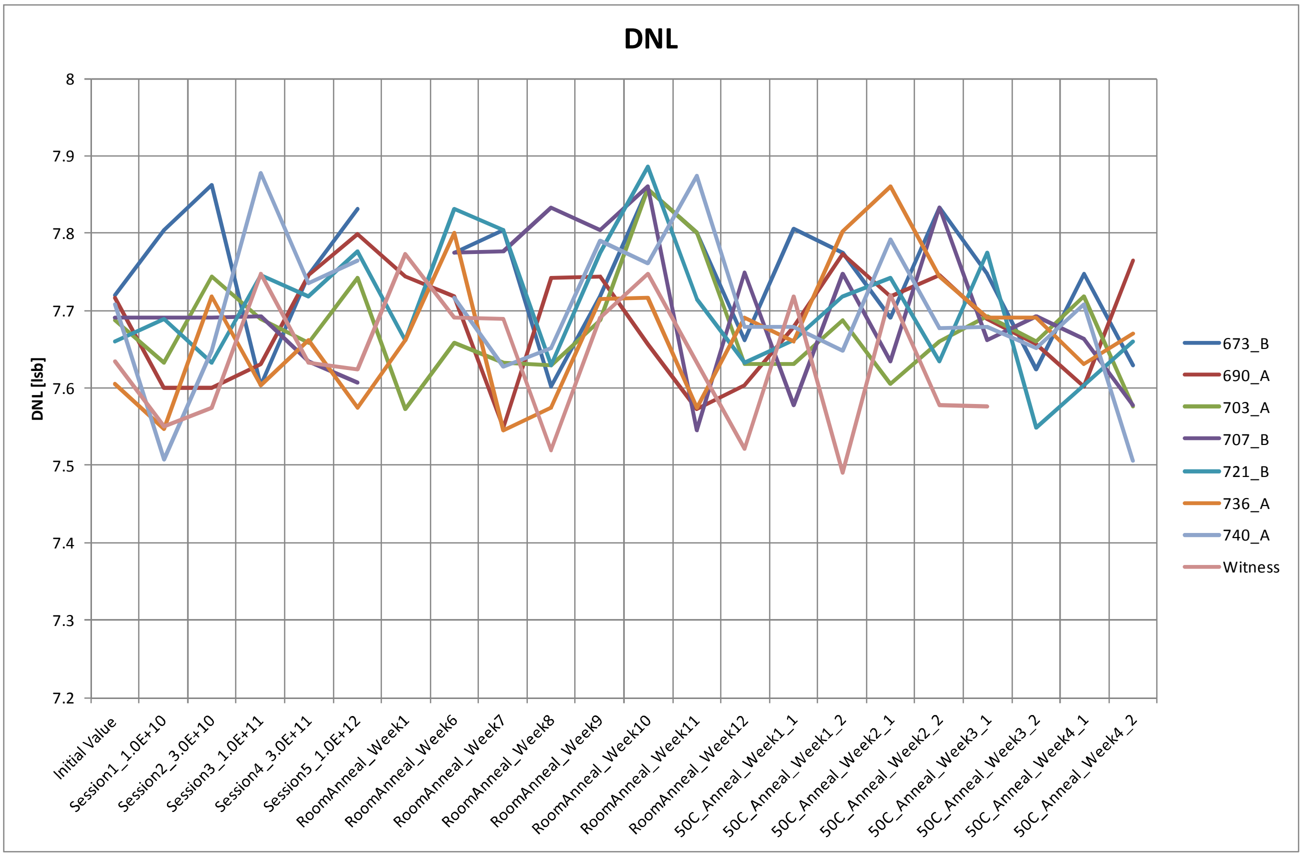

Figure 8-34: DNL vs radiation and annealing

The following observations are made:

- There's no increase or decrease visible during radiation or annealing.

8.2.17.Electro Optical Measurements

The following 2 devices were electrical optical characterized before and after neutron radiation and the corresponding annealing.

Device ID	Silicon Wafer Lot	Lot
690	P29506.1	11-002
703	P29506.1	11-002
164	Reference Device used during HAS2 ESA Eval campaign	

8.2.17.1.Spectral Response

Spectral response could not be measured after 125 degrees annealing due to leakage current in the test photo diode array. The measurements after radiation and annealing clearly shows a degradation in quantum efficiency.

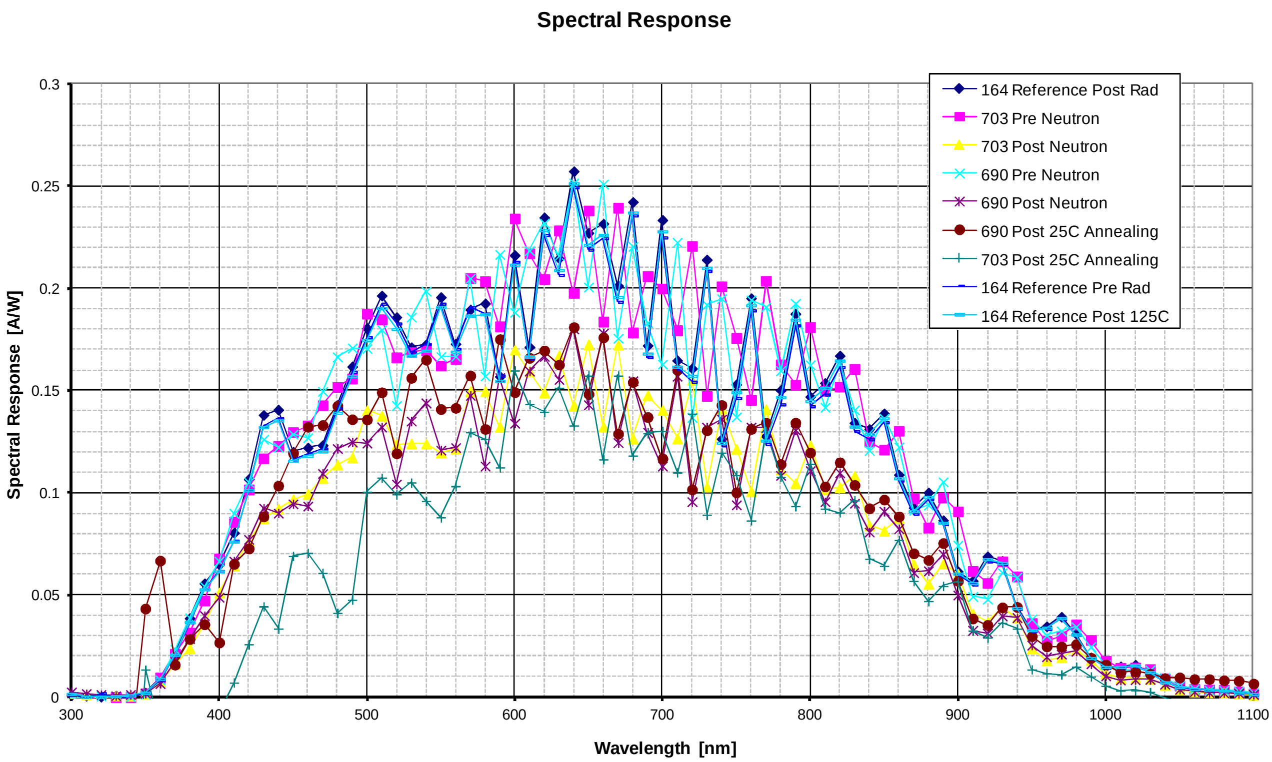

Figure 8-35: Spectral Response Overview

Figure 8-36: Quantum Efficiency device 703

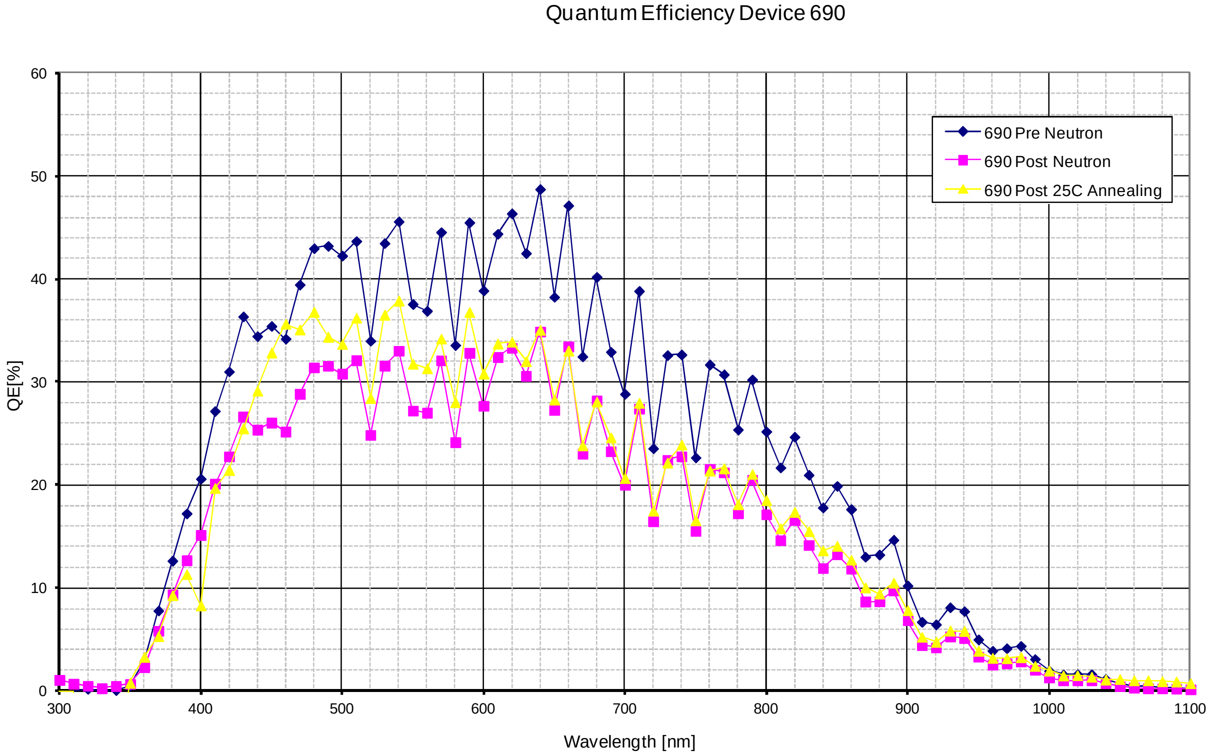

Figure 8-37: Quantum Efficiency device 690

8.2.17.2. Optical Response

The optical response could not be measured after 25 and 125 degrees annealing due to increased leakage currents in the test pixel array.

8.2.17.3. MTF

MTF				
Device	MTF [%] Pre Neutron	MTF [%] Post Neutron	MTF [%] Post 25C Annealing	MTF [%] Post 125C Annealing
690	44.3	42.3	42.8	41.9
703	40.6	43.7	45.1	42.3
164	42.9	40.2	42.8	41.5

The MTF variations are due to setup to setup mismatch. MTF is not changing after neutron irradiation nor annealing.

8.2.17.4. Dark Current Doubling Temperature

Dark Signal Data				
Device	DT [ºC] Pre Neutron	DT [ºC] Post Neutron	DT [ºC] Post 25C Annealing	DT [ºC] Post 125C Annealing
690	5.85	5.48	5.63	12.34
703	5.62	6.05	5.63	11.67
164	5.42	5.31	4.93	5.17

Dark current doubling temperature is unaffected by the radiation and room temperature annealing. After high temperature annealing the doubling temperature has increased significantly. The reason for this behavior is unknown. The same effect has been observed on the TID irradiated parts (both parts were also in the ON state during annealing).

8.2.17.5. Image Lag

Image Lag Data				
Device	Image Lag [%] Pre Neutron	Image Lag [%] Post Neutron	Image Lag [%] Post 25C Annealing	Image Lag [%] Post 125C Annealing
690	1.07	-0.30	-0.38	0.38
703	1.08	-0.27	-0.38	0.46
164	1.07	1.01	0.99	1.29

As expected, image lag is increasing after radiation and is getting worse after radiation. The 50 degrees annealing has no effect on the image lag, instead it even get worse. But this might be due to teh setup to setup variations. After the high temprature annealing, the image lag is slightly heading to its initial value.

8.2.18. Calibration Parameters

Odd/even offset matching, NDR black level offset and temperature sensor curve calibration parameters were measured before and after radiation. As can been seen there is no difference seen before and after radiation. The small differences are due to test-to-test variation. Parameters are not measured anymore after annealing as there were no changes noticed after radiation.

Device Number	Matchable	Value		Black Offset Reg	Temp Calib	Voltage
					85	1.1498
					-40	1.6794
736	0	Not Matchable		26	25	1.4295
					85	1.152
					-40	1.668
736	0	Not Matchable		22	25	1.421
		164	9.79		85	1.1425
		163	16.34		-40	1.6683
703	1	165	1.227	31	25	1.4179
		166	30.15		85	1.154
		165	36.28		-40	1.653
703	1	167	24.32	28	25	1.424
		67	6.201		85	1.1563
		66	15.15		-40	1.682
721	1	68	3.552	28	25	1.4292
		69	1.091		85	1.185
		68	7.117		-40	1.654
721	1	70	6.434	24	25	1.441
		100	3.997		85	1.1447
		99	1.347		-40	1.682
673	1	101	11.99	33	25	1.4262
		101	1.074		85	1.153
		100	12.61		-40	1.658
673	1	102	6.914	30	25	1.435
					85	1.125
					-40	1.6654
707	0	Not Matchable		34	25	1.4112
					85	1.138
					-40	1.674
707	0	Not Matchable		26	25	1.421
					85	1.1296
					-40	1.6603
740	0	Not Matchable		34	25	1.4069
					85	1.175
					-40	1.621
740	0	Not Matchable		31	25	1.408

9.CONCLUSIONS

7 samples were irradiated with neutrons with an equivalent fluence level of 1.0E+12/cm^2 of 10 MeV protons. In order to obtain the value at 1MeV equivalent energy a 3.9 scaling factor is applied.

Due to the available test location, we were not able to bias the devices during irradiation. Instead all devices were irradiated with all their pins grounded.

The following electrical test parameters were affected by the neutrons:

1. Dark current is increasing with neutron radiation. The spread between the devices is almost negligible (this is not the case for TID irradiated devices). Bias conditions (ON/OFF) have no influence on the dark current behavior during annealing. Dark current is decreasing during room, 50C and 125C annealing independent from the bias condition.

2. DSNU trend is the same as for dark current.

3. Sensitivity is dropping with increasing neutron radiation. This results in a higher global and local PRNU (because PRNU is calculated as a percentage of the average grey level).

4. Temporal noise in NDR is increasing with neutron radiation. This is due to the fact that the minimal integration time for an NDR image is 200ms. The DC component is affecting the temporal noise

5. FPN in hard to soft reset is increasing till the 4th radiation cycle, to drop again after the 5th cycle and to come back to its initial value during room temperature annealing. See page 38/40 for detailed explanation.

6. All the FPN measurements are increasing a few percents over time. There's no explanation for this behavior.

The following electro optical parameters were affected by the neutrons:

1. Quantum efficiency is decreasing with increasing radiation.

2. The spectral response diode is affected by leakage so it is not usable anymore for measurements.

3. The dark current doubling temperature increases significantly after 125C degrees annealing. The reason for this behavior is unknown. The same effect has been observed on the TID irradiated parts (both parts were also in the ON state during annealing).